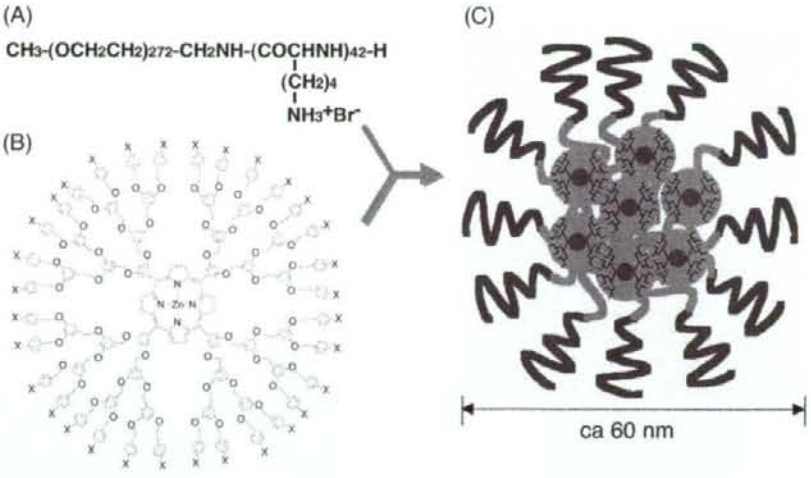

FIGURE 1. Schematic structure of polymeric micelle encapsulating DP. Chemical structures of poly(ethylene glycol) (PEG)-*b*-poly(L-lysine) (**A**) and ionic dendrimer porphyrin (X = COO^-) (DP) (**B**). DP-micelle is spontaneously formed through the electrostatic interaction between PEG-*b*-poly(L-lysine) and DP (**C**).

formulations and their efficacy of PDT in an experimental corneal neovascularization model in mice.

MATERIALS AND METHODS

Animals and Experimental Corneal Neovascularization

Eight-week-old male C57 BJ/6 mice were maintained with free access to food and water. All procedures were performed in accordance with the ARVO Statement for the Use of Animals in Ophthalmic and Vision Research. Animals were placed under general anesthesia by the administration (1.5 mL/kg) of a mixture of ketamine hydrochloride (Ketalar; Sankyo, Tokyo, Japan) and xylazine hydrochloride (Celactal; Bayer, Tokyo, Japan). Corneal neovascularization was induced by suturing 10-0 nylon 1 mm away from limbal vessel under microscopy. Erythromycin ophthalmic ointment was instilled immediately after the procedure.

Photosensitizers

In this study, a third-generation aryl ether dendrimer zinc porphyrin with 32 carboxyl groups on the periphery (DP) and polymeric micelles composed of the DP and PEG-*b*-poly(L-lysine) (DP-micelle) were used for PDT as a PS formulation (Fig. 1). The DP-micelle was prepared according to a previous report.[11] Both DP and DP-micelle have a maximum excitation wavelength at 433 nm. DP-micelle showed 130- to 280-fold higher photocytotoxicity against murine Lewis lung carcinoma cells compared with free DP.[11]

Accumulation of DP and DP-Micelle in Corneal Neovascularization Lesions

Four days after suture placement, DP or DP-micelle was administered by intravenous injection at the dose of 10 mg/kg, again under general anesthesia. Mice were killed 1, 4, 24, and 168 hours after the injection of PS. Before the kill, mice received intravenous BS-1 lectin conjugated with FITC (500 μg/g; Vector Laboratories, Burlingame, CA) to trace the corneal neovascularization area. Corneas were excised and flat-mounted on glass slides. Accumulations of DP or DP-micelle in vascularized areas were observed by fluorescence microscopy (Leica, Deerfield, IL) using 436-nm excitation wavelength. Fluorescence intensities were calculated using NIH Image software and were normalized by traced vascularized areas.

Photodynamic Therapy

Twenty-four hours after DP-micelle or free DP, 38 mice were treated with a diode laser (in-house built laser equipment; Topcon, Tokyo, Japan) of 438-nm wavelength at 500 mW/cm^2 for 20 or 100 seconds, for a total dose of 10 or 50 J/cm^2. The spot size was 1 mm in diameter. As controls, six mice with corneal neovascularization were irradiated without administration of photosensitizers (total dose, 50 J/cm^2). Fluorescein angiography was performed before and 7 days after treatment, and the area of corneal neovascularization was quantified using NIH Image software before and 7 days after irradiation. We defined residual ratio as follows: Residual ratio = (neovascularization area 7 days after irradiation/neovascularization area before irradiation) $\times$ 100%.

RESULTS

Accumulation of DP and DP-Micelle in Corneal Neovascularization Lesions

One hour after the administration of DP-micelle, fluorescence started to accumulate in the neovascularized area and increased until 24 hours after administration (Figs. 2A–C). DP-micelle accumulation decreased but continued after 168 hours (data not shown). After DP administration, fluorescence of DP was observed in the corneal neovascularization area, but it was weaker than that of DP-micelle group (Figs. 2D-F) and disappeared by 168 hours (data not shown). Figure 3 shows the time course of normalized fluorescence intensities of DP in the neovascularized area. DP-micelle intensities were significantly higher than those of free DP 1 hour (n = 7/each condition), 4 hours (n = 6/each condition), and 24 hours (n = 6/each condition) after administration (P = 0.032, 0.047, 0.0066; Mann-Whitney U test). Neither DP-micelle nor free DP could be detected microscopically in normal limbal vasculature or other ocular tissue such as iris, retina, and conjunctiva (data not shown).

Photodynamic Therapy

Figure 4 is a series of fluorescence angiographic images of corneal neovascularization before and 7 days after PDT in the control, DP-micelle, and DP groups. As shown in Figure 4A, there was no effect of irradiation in the control (n = 6). Seven days after irradiation at 10 J/cm^2, the mean residual ratio of

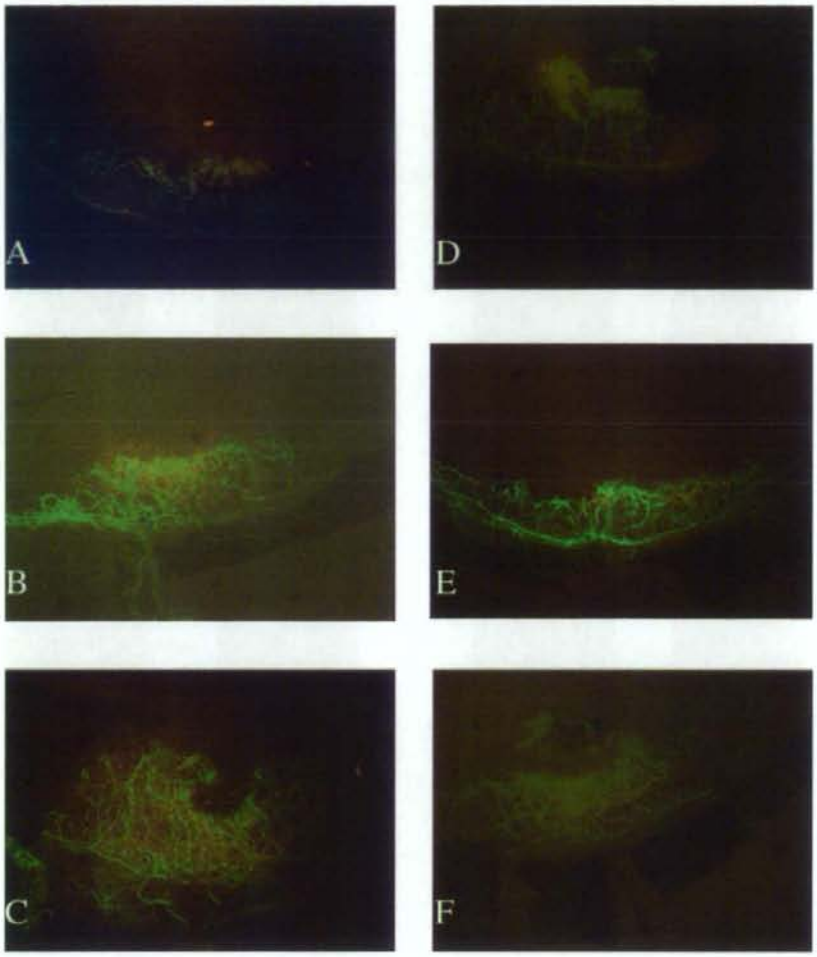

FIGURE 2. Accumulation of DP and DP-micelle to neovascularized area. The flatmounts of the neovascularization area were observed under a fluorescent microscope 1 hour (**A**), 4 hours (**B**), and 24 hours (**C**) after administration of DP-micelle and 1 hour (**D**), 4 hours (**E**), and 24 hours (**F**) hours after injection of DP. Vessels were stained with BS-1 lectin conjugated with FITC. Fluorescence of DP was observed 1 hour after administration (**A**, **D**) and enhanced until 24 hours after.

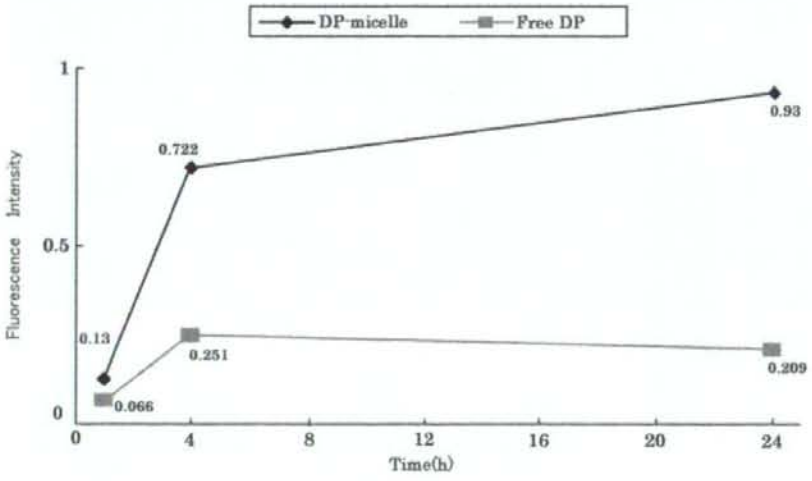

FIGURE 3. Time course of fluorescence intensity. Fluorescence intensity of DP in cornea after administration of DP-micelle or free DP. Fluorescence of DP was detected in the corneas of the DP-micelle group as early as 1 hour, and intensity reached a peak 24 hours after intravenous administration, whereas the intensity in the free DP group was significantly lower than that in the DP-micelle group.

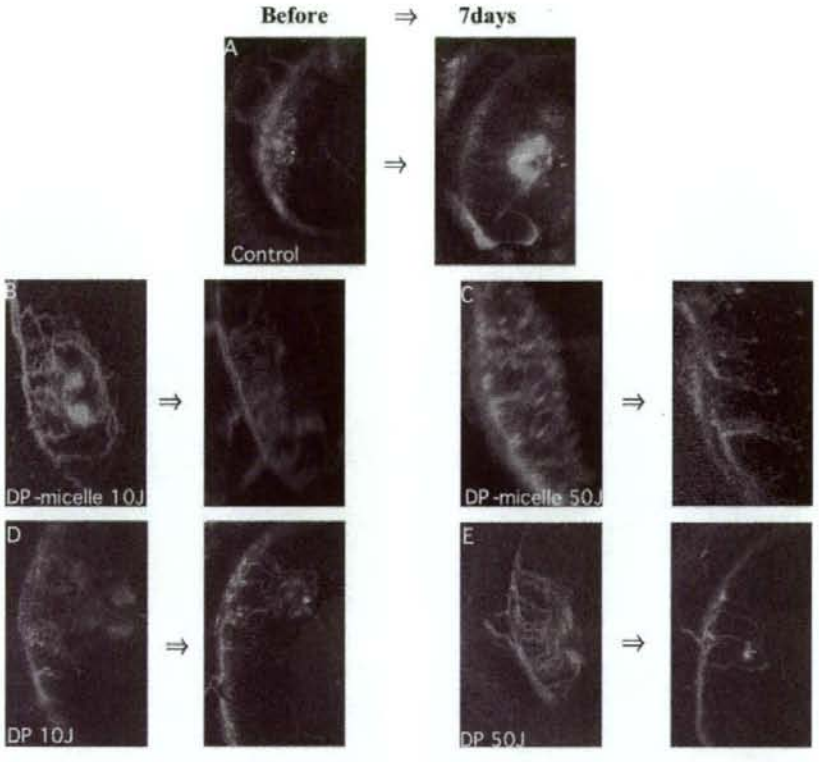

FIGURE 4. Neovascularization regression after PDT. (**A**) Control. No regression was observed without micelle or DP administration. (**B**) Irradiation at 10 J/cm^2 with DP-micelle. (**C**) 50 J/cm^2 with DP-micelle. (**D**) Irradiation at 10 J/cm^2 with DP. (**E**) Irradiation at 50 J/cm^2 with DP. (**B–E**) In each group, significant regression of neovascularization was observed.

corneal neovascularization was 10.1% in the mice treated with DP-micelle (n = 9) and 21.6% in the mice treated with free DP (n = 10; Fig. 5). The residual ratio of mice treated with DP-micelle was significantly higher than that of mice treated with free DP ($P < 0.01$; Mann-Whitney U test). Seven days after irradiation at 50 J/cm^2, the mean residual area of corneal neovascularization was 10.6% in the mice treated with DP-micelle (n = 10) and 13.7% in the mice treated with free DP (n = 9; $P > 0.05$; Mann-Whitney U test; Fig. 5). Histologic examination after PDT showed no injury on corneal tissue (data not shown).

DISCUSSION

PDT potentially represents a new approach for the treatment of neovascular disease and tumor.[14] The successful treatment of choroidal neovascularization by PDT opens the possibility of treating other neovascular diseases of the eye, including the cornea, in a similar manner.[15–17] Indeed, several past studies revealed that PDT was efficacious for the treatment of corneal neovascularization.[18–21]

One of ideal characteristics of PS is selectivity to neovasculature. In this study, DP-micelle, a newly developed PS

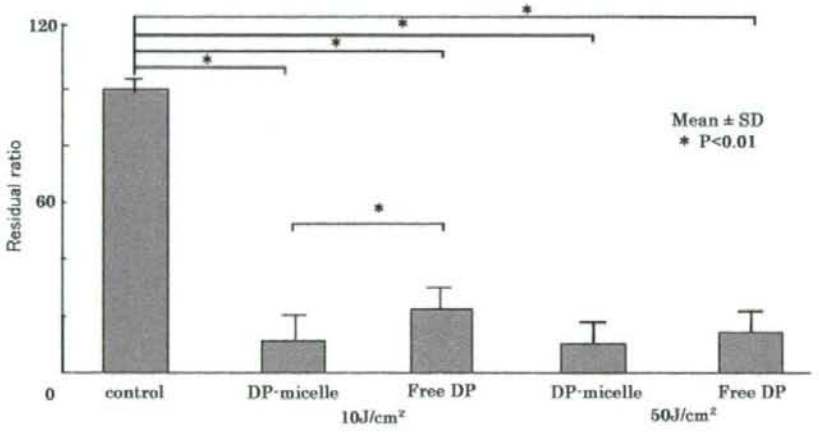

FIGURE 5. Residual ratio of corneal neovascularization 7 days after PDT. Residual ratio of corneal neovascularization 7 days after PDT with DP-micelle or DP or with no administration. Residual ratios were 10.1% with irradiation at 10 J/cm^2 and micelle, 21.6% with irradiation at 10 J/cm^2 and DP, 10.6% with irradiation at 50 J/cm^2 and micelle, and 13.7% with irradiation at 10 J/cm^2 and DP. Error bars indicate SD.

FIGURE 6. Long-term effect of PDT. (A) Before irradiation. (B) Seven days after irradiation at 10 J/cm^2 with micelle. Significant regression of neovascularization was observed. (C) Sixty-three days after irradiation. Little recanalization of neovascularization was observed, but a few matured vessels were not occluded.

formulation, was accumulated only in pathologic vascularized areas. On the other hand, DP-micelle and free DP were not detectable in normal vessel areas, including other ocular vessels (data not shown). The high selectivity of these PSs to neovascularization should result in minimal side effects in the adjacent normal corneal structure. Indeed, slit lamp examination and histologic observation showed no alterations by PDT to the surrounding structure, including epithelium, stroma, and endothelium (data not shown).

Macromolecular compounds can accumulate and prolong their retention in the perivascular regions of solid tumors to a greater extent than in normal tissues because newly formed vessels in solid tumors exhibit higher substance permeability than in normal tissues and because lymph systems in tumor tissue are incomplete. This effect is known as the enhanced permeability retention (EPR) effect.[22] We have demonstrated that polymeric micelles with diameters of several tens of nanometers with narrow distribution can accumulate in a solid tumor though the EPR effect.[23–25]

As do solid tumors, corneal neovascularization sites appear to have high permeability and incomplete lymph systems. Hence, we assume that DP-micelle can accumulate selectively in corneal neovascularization lesions.

Another ideal characteristic in PDT is high photocytotoxicity with lower dark cytotoxicity. As reported earlier, the laser energy of PDT for corneal neovascularization with verteporphin, a PS used clinically for choroidal neovascularization, was 150 J/cm^2 to create long-lasting clinical regression of corneal neovasculature.[19] This is three times the amount needed to create regression of choroidal neovascularization. PDT with DP-micelle required only 10 J/cm^2 for long-lasting regression of neovascularization. Most PSs have hydrophobic properties resulting in their self-quenching from aggregation, decreasing photooxidation efficacy to achieve successful PDT. Dendrimer photosensitizers are designed to prevent the aggregation of core PS even in the micellar core. In addition to the EPR effect, this property might have led to a higher neovascularization regression rate in our study than in past studies.

This study indicates PDT with DP-micelle and free DP can provide efficacious treatment of corneal neovascularization. It is important to observe and examine the long-term effects in the future. We observed 2 months after irradiation with PIC micelle at laser energies of 10 J/cm^2. As shown in Figure 6, most of the corneal neovasculature was not recanalized, though a few matured vessels remained over 2 months. In addition, polymeric micelles can encapsulate a variety of drugs, including hydrophobic substances, nucleic acids, and proteins in the core[23]; therefore, they have great potential for effective drug delivery targeting to corneal neovascularization.

References

1. Lee P, Wang CC, Adamis AP. Ocular neovascularization an epidemiologic review. *Surv Ophthalmol*. 1998;43:245–269.
2. Williams KA, Esterman AJ, Barlett C, Holland H, Hornsby NB, Coster DJ. How effective is penetrating corneal transplantation? Factors influencing long-term outcome in multivariate analysis. *Transplantaion*. 2006;81:896–901.
3. Epstein RJ, Stulting RD, Hendricks RL, Harris DM. Corneal neovascularization: pathogenesis and inhibition. *Cornea*. 1987;6:250–257.
4. Marsh RJ, Marshall J. Treatment of lipid keratopathy with the argon laser. *Br J Ophthalmol*. 1982;66:127–135.
5. Mendelsohn AD, Stock EL, Lo GG, et al. Laser photocoagulation of feeder vessels in lipid keratopathy. *Ophthalmic Surg*. 1986;17:502–508.
6. Nirankari VS, Baer JC. Corneal argon laser photocoagulation for neovascularization in penetrating keratoplasty. *Ophthalmology*. 1986;93:1304–1309.
7. Marsh RJ. Argon laser treatment of lipid keratopathy. *Br J Ophthalmol*. 1988;72:900–904.
8. Lai CM, Spilsbury K, Brankov M, Zaknich T, Rakoczy PE. Inhibition of corneal neovascularization by recombinant adenovirus mediated antisense VEGF RNA. *Exp Eye Res*. 2002;75:625–634.
9. Brooks BJ, Ambati BK, Marcus DM, Ratanasit A. Photodynamic therapy for corneal neovascularization and lipid degeneration. *Br J Ophthalmol*. 2004;88:840.
10. Nishiyama N, Stapert RH, Zahng GD, et al. Light-harvesting ionic dendrimer porphyrins as new photosensitizers for photodynamic therapy. *Bioconjug Chem*. 2003;14:58–66.
11. Jang WD, Nishiyama N, Zhang GD, et al. Supramolecular nanocarrier of anionic dendrimer porphyrins with PEGylated cationic block copolymer to enhance intracellular photodynamic efficacy. *Angew Chem Int Ed*. 2005;44:419–423.
12. Ideta R, Tasaka F, Jang WD, et al. Nanotechnology-based photodynamic therapy for neovascular disease using a supramolecular nanocarrier loaded with a dendritic photosensitizer. *Nano Lett*. 2005;5:2426–2431.
13. Usui T, Sugisaki K, Amano S, Jang WD, Nishiyama N, Kataoka K. New drug delivery for corneal neovascularization using polyion complex micelles. *Cornea*. 2005;24:S39–S42.
14. Awan MA, Rarin SA. Review of photodynamic therapy. *Surgeon*. 2006;4:231–236.
15. Harding S. Photodynamic therapy in the treatment of subfoveal choroidal neovascularization. *Eye*. 2001;15:407–412.
16. Verteporfin in Photodynamic Therapy Study Group. Photodynamic therapy of subfoveal choroidal neovascularization in pathologic myopia with verteporfin. 1-year results of a randomized clinical trial—VIP report no. 1. *Ophthalmology*. 2001;108:841–852.

17. Photodynamic therapy of subfoveal choroidal neovascularization in age-related macular degeneration with verteporfin: one-year results of 2 randomized clinical trials—TAP report: Treatment of Age-Related Macular Degeneration with Photodynamic Therapy (TAP) Study Group. *Arch Ophthalmol.* 1999;117:1329–1345.
18. Gohto Y, Obana A, Kaneda K, Miki T. Photodynamic effect of a new photosensitizer ATX-S10 on corneal neovascularization. *Exp Eye Res.* 1998;67:213–322.
19. Holtzer MP, Solomon KD, Vroman DT, et al. Photodynamic therapy with verteporfin in a rabbit model of corneal neovascularization. *Invest Ophthalmol Vis Sci.* 2003;44:2954–2958.
20. Fossarello M, Peiretti E, Zucca I, Serra A. Photodynamic therapy of corneal neovascularization with verteporfin. *Cornea.* 2003;22:485–488.
21. Sawa M, Awazu K, Takahashi T, et al. Application of femtosecond ultrashort pulse laser to photodynamic therapy mediated by indocyanine green. *Br J Ophthalmol.* 2004;88:826–831.
22. Matumura Y, Maeda H. A new concept for macromolecular therapeutics in cancer chemotherapy: mechanism of tumoritropic accumulation of proteins and the antitumor agent SMANCS. *Cancer Res.* 1986;46:6387–6392.
23. Nishiyama N, Kataoka K. Current state, achievements, and future prospects of polymeric micelles as nanocarriers for drug and gene delivery. *Pharmacol Ther.* 2006;112:630–648.
24. Bae Y, Nishiyama N, Fukushima S, Koyama H, Matsumura Y, Kataoka K. Preparation and biological characterization of polymeric micelle drug carriers with intracellular pH-triggered drug release property: tumor permeability, controlled subcellular drug distribution, and enhanced in vivo antitumor efficacy. *Bioconjugate Chem.* 2005;16:122–130.
25. Nishiyama N, Okazaki S, Cabral H, et al. Novel cisplatin-incorporated polymeric micelles can eradicate solid tumors in mice. *Cancer Res.* 2003;63:8977–8983.

Journal of Controlled Release 133 (2009) 198–205

Contents lists available at ScienceDirect

Journal of Controlled Release

journal homepage: www.elsevier.com/locate/jconrel

A novel strategy utilizing ultrasound for antigen delivery in dendritic cell-based cancer immunotherapy

Ryo Suzuki [a], Yusuke Oda [a], Naoki Utoguchi [a], Eisuke Namai [a], Yuichiro Taira [a], Naoki Okada [b], Norimitsu Kadowaki [c], Tetsuya Kodama [d], Katsuro Tachibana [e], Kazuo Maruyama [a,*]

[a] Department of Biopharmaceutics, School of Pharmaceutical Sciences, Teikyo University, 1091-1 Suwarashi, Sagamiko-cho, Sagamihara, Kanagawa 229-0195, Japan
[b] Department of Biotechnology and Therapeutics, Graduate School of Pharmaceutical Sciences, Osaka University, 1-6 Yamadaoka, Suita, Osaka 565-0871, Japan
[c] Department of Hematology and Oncology, Graduate School of Medicine, Kyoto University, 54 Shogoin Kawara-cho, Sakyo-ku, Kyoto 606-8507, Japan
[d] Department of Biomedical Engineering, Graduate School of Biomedical Engineering, Tohoku University, 2-1 Seiryo-machi, Aoba-ku, Sendai 980-8575, Japan
[e] Department of anatomy, School of medicine, Fukuoka University, 7-45-1 Nanakuma, Jonan-ku, Fukuoka 814-0180, Japan

ARTICLE INFO

Article history:
Received 12 August 2008
Accepted 16 October 2008
Available online 31 October 2008

Keywords:
Dendritic cells
Antigen delivery system
Cancer immunotherapy
Ultrasound
Liposomes

ABSTRACT

In dendritic cell (DC)-based cancer immunotherapy, it is important that DCs present peptides derived from tumor-associated antigens on MHC class I, and activate tumor-specific cytotoxic T lymphocytes (CTLs). However, MHC class I generally present endogenous antigens expressed in the cytosol. We therefore developed an innovative approach capable of directly delivering exogenous antigens into the cytosol of DCs; i.e., a MHC class I-presenting pathway. In this study, we investigated the effect of antigen delivery using perfluoropropane gas-entrapping liposomes (Bubble liposomes, BLs) and ultrasound (US) exposure on MHC class I presentation levels in DCs, as well as the feasibility of using this antigen delivery system in DC-based cancer immunotherapy. DCs were treated with ovalbumin (OVA) as a model antigen, BLs and US exposure. OVA was directly delivered into the cytosol but not via the endocytosis pathway, and OVA-derived peptides were presented on MHC class I. This result indicates that exogenous antigens can be recognized as endogenous antigens when delivered into the cytosol. Immunization with DCs treated with OVA, BLs and US exposure efficiently induced OVA-specific CTLs and resulted in the complete rejection of E.G7-OVA tumors. These data indicate that the combination of BLs and US exposure is a promising antigen delivery system in DC-based cancer immunotherapy.

1. Introduction

Dendritic cells (DCs), which are unique antigen-presenting cells capable of priming naive T cells, are promising vaccine carriers for cancer immunotherapy [1]. To induce efficiently a tumor-specific cytotoxic T-lymphocyte (CTL) response, DCs should abundantly present epitope peptides derived from tumor-associated antigens (TAAs) via major histocompatibility complex (MHC) class I molecules [2]. In general, the majority of peptides presented via the MHC class I molecules are generated from endogenously synthesized proteins that are degraded by the proteasome [3]. On the other hand, exogenous antigens such as TAAs for DCs are preferentially presented on MHC class II molecules [3]. In order to prime efficiently TAAs specific for CTLs, it is important to develop a novel antigen delivery system, which can induce MHC class I restricted TAA presentation on DCs. Several researchers are developing antigen delivery tools based on the cross presentation theory of exogenous antigens for DCs [4–8]. In these studies, various types of antigen delivery carriers such as liposomes [6,7], poly(γ-glutamic acid) nanoparticles [5] and cholesterol pullulan nanoparticles [8], all of which can deliver antigen into DCs via the endocytosis pathway, have been developed. We have reported that IgG modified liposomes with entrapped antigen can induce cross presentation of exogenous antigen for DCs on MHC class I molecules [9]. These carriers deliver antigens into DCs via an endocytosis mechanism, with delivery thought to be due to exogenous antigen leaking from the endosome into the cytosol. It is therefore important to design an antigen delivery system which does not rely on the endocytosis pathway. In other study, it was reported that DCs pulsed with exogenous antigens by electroporation presented their antigens on MHC class I molecules and resulted

Abbreviations: Alexa-OVA, Alexa Fluor 488-conjugated ovalbumin; BL, Bubble liposome; CTL, cytotoxic T lymphocyte; DC, dendritic cell; DSPC, 1,2-distearoyl-sn-glycero-phosphatidylcholine; DSPE-PEG(2k)-OMe, 1,2-distearoyl-sn-glycero-3-phosphatidyl-ethanolamine-methoxypolyethyleneglycol; ER, endoplasmic reticulum; FBS, fetal bovine albumin; HLA, human leukocyte antigen; MHC, major histocompatibility complex; MTT, 3-(4,5-s-dimethylthiazol-2-yl)-2,5-diphenyl tetrazolium bromide; NaN_3, sodium azide; OVA, ovalbumin; PBS, phosphate buffer saline; US, ultrasound; TAA, tumor associated antigen.

* Corresponding author. Department of Biopharmaceutics, School of Pharmaceutical Sciences, Teikyo University, 1091-1 Suwarashi, Sagamiko-cho, Sagamihara, Kanagawa 229-0195, Japan. Tel.: +81 42 685 3722; fax: +81 42 685 3432.
E-mail address: maruyama@pharm.teikyo-u.ac.jp (K. Maruyama).

0168-3659/$ – see front matter © 2008 Elsevier B.V. All rights reserved.
doi:10.1016/j.jconrel.2008.10.015

in inducing MHC class I-mediated antitumor immunity. Although electroporation is commonly utilized as gene delivery method and deliver gene such as DNA and RNA into cytosol, Kim K.W. et al and Weiss J.M. et al. apply this system to antigen delivery into DCs [10,11]. Their reports also demonstrate the importance of delivering exogenous antigens into cytosol of DCs to induce MHC class I presentation of the antigens.

It has been reported that ultrasound (US) increases the permeability of the plasma membrane, which encourages the entry of DNA into cells [12,13]. The first studies applying US for gene delivery used frequencies in the range of 20–50 kHz [12,14]. However, these frequencies, along with cavitation, are also known to induce tissue damage if not properly controlled [15–17]. To address this problem, many studies into using therapeutic US for gene delivery have used frequencies of 1–3 MHz, intensities of 0.5–2.5 W/cm^2 and a pulse-mode [18–20]. In addition, it was reported that the combination of therapeutic US and microbubble echo contrast agents could enhance gene transfection efficiency [21–27]. In this method, DNA is effectively and directly transferred into the cytosol. This system has been applied to deliver proteins into cells [28,29], but not yet to deliver antigens into DCs for the purpose of cancer immunotherapy. Previously, we developed novel liposomal bubbles containing nanobubbles of the US imaging gas, perfluoropropane [30–34] and suggested that these "Bubble liposomes" (BLs) might be used as novel non-viral gene delivery tools if combined with US exposure. In the case of DCs, the antigen delivered into the cytosol would present on MHC class I molecules and result in priming antigen-specific CTLs. In this study, we examined the effectiveness of BLs combined with US exposure to deliver antigen into DCs. In addition, the effectiveness of this antigen delivery system in DC-based cancer immunotherapy was assessed.

2. Materials and methods

2.1. Cells

T cell hybridoma CD8-OVA1.3 (a kind gift from Dr. C.V. Harding, Department of Pathology, Case Western Reserve University, Cleveland, OH, USA), a cell type that recognizes SIINFEKL:H-2K^b complexes [35], was cultured in Dulbecco's modified Eagle's medium (DMEM, Sigma Chemical Co., St. Louis, MO, USA) supplemented with 10% heat inactivated fetal bovine serum (FBS, GIBCO, Invitrogen Co., Carlsbad, CA, USA), 50 μM 2-mercaptethanol (2-ME), 250 μg/ml amphotericin B (Wako Pure Chemical Industries, Ltd., Osaka, Japan) and 50 μg/ml gentamycin (Wako Pure Chemical Industries). EL-4 murine thymoma cells were cultured in RPMI 1640 supplemented with 10% FBS and 50 μM 2-ME. E.G7-OVA cells (OVA cDNA transfectant of EL4 cells) were maintained in RPMI 1640 supplemented with 10% FBS, 50 μM 2-ME and 400 μg/ml GENETICIN (G418 sulfate, GIBCO, Invitrogen). All culture media contained 50 U/ml penicillin and 50 μg/ml streptomycin (Wako Pure Chemical Industries).

2.2. Generation of mouse bone marrow-derived DCs

DCs were generated from bone marrow cells as described elsewhere [36]. Briefly, bone marrow cells were isolated from C57BL/6 mice and were cultured in RPMI 1640 with 10% FBS, 50 U/ml penicillin, 50 μg/ml streptomycin and 40 ng/ml mouse granulocyte-macrophage colony-stimulating factor (GM-CSF). After 8–16 days of culture, non-adherent cells were collected and used as DCs.

2.3. Preparation of BLs

Liposomes composed of 1,2-distearoyl-sn-glycero-phosphatidylcholine (DSPC) (NOF Corp., Tokyo, Japan) and 1,2-distearoyl-sn-glycero-3-phosphatidyl-ethanolamine-methoxypolyethyleneglycol (DSPE-PEG(2k)-OMe, (PEG Mw≈ca. 2000), NOF) (94 : 6 (m/m)) were prepared by reverse phase evaporation. Briefly, all reagents (total lipid: 100 μmol) were dissolved in 8 ml of 1:1 (v/v) chloroform/diisopropyl ether, then 4 ml of phosphate buffered saline (PBS) was added. The mixture was sonicated and evaporated at 65 °C. The solvent was completely removed, and the size of the liposomes was adjusted to less than 200 nm using an extruding apparatus (Northern Lipids Inc., Vancouver, BC, Canada) and sizing filters (pore sizes: 100 and 200 nm; Nuclepore Track-Etch Membrane, Whatman plc, UK). After sizing, the liposomes were sterilized by passing them through a 0.45 μm pore size filter (MILLEX HV filter unit, Durapore PVDF membrane, Millipore Corp., MA, USA). The size of the liposomes was measured by dynamic light scattering (ELS-800, Otsuka Electronics Co., Ltd., Osaka, Japan). The average diameter of these liposomes was between 150–200 nm. Lipid concentration was measured using the Phospholipid C test (Wako Pure Chemical Industries). BLs were prepared from the liposomes and perfluoropropane gas (Takachiho Chemical Industrial Co., Ltd., Tokyo, Japan) [31,33]. Briefly, 5 ml sterilized vials containing 2 ml of the liposome suspension (lipid concentration: 2 mg/ml) were filled with perfluoropropane, capped, and then supercharged with 7.5 ml of perfluoropropane. The vial was placed in a bath-type sonicator (42 kHz, 100 W; BRANSONIC 2510J-DTH, Branson Ultrasonics Co., Danbury, CT, USA) for 5 min to form the BLs. In this method, the liposomes were reconstituted by sonication under the condition of supercharge with perfluoropropane in the 5 mL vial container. At the same time, perfluoropropane would be entrapped within lipids like micelles, which were made by DSPC and DSPE-PEG(2k)-OMe from liposome composition, to form nanobubbles. The lipid nanobubbles were encapsulated within the reconstituted liposomes, which sizes were changed into around 1 μm from 150–200 nm of original.

2.4. Antigen trafficking into DCs after antigen delivery with BLs and US exposure

Alexa Fluor 488 conjugated OVA (Alexa-OVA) was prepared with Alexa Fluor 488 succinimidyl ester (Molecular Probes, Invitrogen) according to the instruction manual. DCs (1×10^5 cells/ml) were cultured in a glass bottom dish (IWAKI, Asahi Glass Co. Ltd., Tokyo, Japan) overnight. After washing the cells with OptiMEM (Invitrogen), BLs (240 μg/ml) and Alexa-OVA (50 μg/ml) were added to the dish. Then, the DCs were exposed to US exposure (frequency: 2 MHz, duty: 10%, burst rate: 2.0 Hz, intensity 2.0 W/cm^2, time: 3×10 s (interval: 10 s)) using a Sonopore 4000 (6 mm diameter probe; Nepa Gene Co. Ltd., Chiba, Japan). This condition was decided referring to our reports about gene delivery [31,33] and Guo et al.'s report about the repeat US exposure with interval [37], and from the viewpoint of cytotoxicity for DCs. After US exposure, the DCs were incubated for 1 h at 37 °C, then washed with PBS, fixed with 3% paraformaldehyde for 10 min, and treated with 0.1% Triton X-100 (Wako Pure Chemical Industries) for 5 min. In addition, some DCs were washed with PBS, their nuclei were stained with propidium iodide (0.5 μg/ml) (Wako Pure Chemical Industries), and antigen trafficking was observed with a confocal laser microscope.

2.5. Antigen delivery following inhibition of the endocytosis pathway in DCs

DCs were pretreated with OptiMEM containing 10 mM NaN_3 for 1 h at 4 °C to inhibit the endocytosis pathway. After washing the cells, BLs (240 μg/ml) and Alexa-OVA (50 μg/ml) were added to the DCs in OptiMEM containing 10 mM sodium azide (NaN_3). The DCs were exposed to US exposure (frequency: 2 MHz, duty: 10%, burst rate: 2.0 Hz, intensity 2.0 W/cm^2, time: 3×10 s (interval: 10 s)), then washed with PBS containing10 mM NaN_3. After US exposure, DCs were fixed and their nuclei were stained as described above (2.4.).

2.6. Flow cytometry analysis of antigen delivery into DCs with BLs and US exposure

Alexa-OVA was delivered into DCs under inhibited endocytosis conditions as described above (2.5.). After washing, the DCs were stained with propidium iodide (100 ng/ml) and analyzed by flow cytometry (FACSCalibur, Becton, Dickinson and Company, Franklin Lakes, NJ, USA). In this study, living DCs (1×10^4 cells) were analyzed by gating out propidium iodide staining cells.

2.7. Assessment of MHC class I restricted OVA presentation

DCs (2.5×10^5 cells/500 μl/well (48-well plate)) were pulsed with OVA alone (0, 10, 100, 1000 μg/ml) or OVA (0, 10, 100, 1000 μg/ml) using US exposure (frequency: 2 MHz, duty: 10%, burst rate: 2.0 Hz, intensity 2.0 W/cm^2, Time: 3×10 s (interval: 10 s)) and/or BLs (240 μg/ml). After US exposure, the DCs were incubated for 1 h at 37 °C, then washed with PBS. After culturing for 24 h, the DCs were co-cultured for 20 h with T cell hybridoma CD8-OVA1.3 (2×10^5 cells/well) that recognizes SIINFEKL: H-2K^b complexes. The concentration of IL-2 in the supernatants was measured using an IL-2 ELISA Kit (BioSource International, Inc., Camarillo, CA, USA).

2.8. Assessment of cytotoxicity to DCs by the treatment of BLs and US exposure

DCs (2.5×10^5 cells/500 μl/well (48-well plate)) were treated with BLs (240 μg/ml) and/or US exposure (frequency: 2 MHz, duty: 10%, burst rate: 2.0 Hz, intensity 2.0 W/cm^2, Time: 3×10 s (interval: 10 s)). After US exposure, DCs were incubated for 1 h at 37 °C, and washed with PBS. The DCs were resuspended with cuture medium (250 μl) and cultured for 48 h. Cell viability was assayed using MTT (3-(4,5-s-dimethylthiazol-2-yl)-2,5-diphenyl tetrazolium bromide, Dojindo, Kumamoto, Japan) as described by Mosmann with minor modifications [38]. Briefly, MTT (5 mg/mL, 25 μL) was added to each well and the cells were incubated at 37 °C for 4 h. The formazan product was dissolved in 250 μL of 10% sodium dodecyl sulfate (SDS, Wako Pure Chemical Ind. Co., Ltd. Osaka, Japan) containing 15 mM HCl. Color intensity was measured using a microplate reader (POWERSCAN HT; Dainippon Pharmaceutical, Osaka, Japan) at test and reference wavelengths of 595 and 655 nm, respectively.

2.9. Immunization of mice with DCs and cytotoxicity assay

DCs (2.5×10^5 cells/500 μl/well) were pulsed with OVA alone (100 μg/ml) or OVA (100 μg/ml) using US exposure (frequency: 2 MHz, duty: 10%, burst rate: 2.0 Hz, intensity 2.0 W/cm^2, Time: 3×10 s (interval: 10 s)) and/or BLs (240 μg/ml) on a 48-well plate, then collected from 10 wells and seeded into 6-well plates. After 1 h incubation at 37 °C, the DCs were washed and cultured for 24 h at 37 °C. After washing, DCs (1×10^6 cells/100 μl) were intradermally injected into the backs of C57BL/6 mice. After 7 days, the mice were re-immunized. Seven days after the second immunization, splenocytes were obtained from five mice, and the splenocytes were pooled and stimulated with mitomycin C-treated E.G7-OVA cells at a ratio of 10:1 for 5 days. The stimulated splenocytes were used as effector cells for the cytotoxicity assay, using EL-4 or E.G7-OVA as the target cells in a flow cytometric assay employing two fluorochromes [39]. PKH-67, a fluorochrome which fluoresces green, binds to the cytoplasmic membrane and does not leak or transfer, was used to identify the target cell population. Propidium iodide fluoresces red and was used to detect non-viable cells. Use of these two fluorochromes and two parameter analyses allowed the identification of four subpopulations in the sample: live effectors, dead effectors, live targets and dead targets. By enumerating these subpopulations, the percent target lysis can be calculated.

2.10. Antitumor effect by prior immunization with antigen-pulsed DCs

DCs (2.5×10^5 cells/500 μl/well) were pulsed with OVA alone (100 μg/ml) or OVA (100 μg/ml) using US exposure (frequency: 2 MHz, duty: 10%, burst rate: 2.0 Hz, intensity 2.0 W/cm^2, Time: 3×10 s (interval: 10 s)) and/or BLs (240 μg/ml) on a 48-well plate, then collected from 10 wells and seeded into 6-well plates. After 1 h incubation at 37 °C, the DCs were washed and cultured for 24 h at 37 °C. After washing, the DCs (1×10^6 cells/100 μl) were intradermally immunized into the backs of C57BL/6 mice twice at intervals of one week. Seven days after the second immunization, E.G7-OVA cells (1×10^6 cells) were intradermally inoculated into the backs of mice and the size of the tumors was monitored using the formula: (major axis×minor axis^2)×0.5. All treated groups contained five mice.

2.11. Re-challenge of tumor cells

E.G7-OVA cells (1×10^6 cells) were injected into mice that were resistant to tumor cells due to immunization with DCs treated with BLs, US exposure and OVA. Untreated mice were used as controls to confirm the development of cancer following the first inoculation with E.G7-OVA cells. All treated groups contained five mice.

2.12. Treatment of tumor-bearing mice with antigen-pulsed DCs

E.G7-OVA cells (1×10^6 cells) were intradermally inoculated into the backs of C57BL/6 mice. On day 9, when the tumors were between 8–10 mm, OVA pulsed DCs (1×10^6 cells) prepared as described above were intradermally injected into the backs of the mice. On day 12, DCs were injected similarly. Tumor sizes were monitored from the day of inoculation. All treated groups contained five mice.

2.13. Statistical analysis

Differences in IL-2 secretion between the experimental groups were compared using non-repeated measures ANOVA and Dunnett's test.

3. Results

3.1. Antigen delivery by BLs and sonoporation into the cytosol of DCs lacking the endocytosis pathway

We examined antigen trafficking following delivery using a combination of BLs and US exposure (Fig. 1(a)). In DCs treated with Alexa-OVA in the presence or absence of either BLs or US exposure, the fluorescence from Alexa-OVA appeared as dots in the cytosol. On the other hand, in DCs treated with Alexa-OVA, BLs and US exposure, the fluorescence appeared as dots, but also as diffused fluorescence in the cytosol. To confirm this, antigen delivery was examined following inhibition of the endocytosis pathway in DCs by treatment with sodium azide (Fig. 1(b)). In DCs treated with Alexa-OVA either with or without BLs or US exposure, the fluorescence derived from Alexa-OVA was not observed. On the other hand, in DCs treated with Alexa-OVA, BLs and US exposure, fluorescence was observed in the cytosol even when the endocytosis pathway in DCs was inhibited. In addition, the efficiency of antigen delivery following inhibition of the endocytosis pathway was assessed using flow cytometory (Fig. 1(c)). The fluorescence intensity of DCs treated with Alexa-OVA, BLs and US exposure was higher than that of DCs treated with Alexa-OVA alone, or of Alexa-OVA and BLs or US exposure. These data support the data shown in Fig. 1(b), indicating that Alexa-OVA is observed in the cytosol when DCs are only treated with BLs and US exposure, even when the endocytosis pathway is

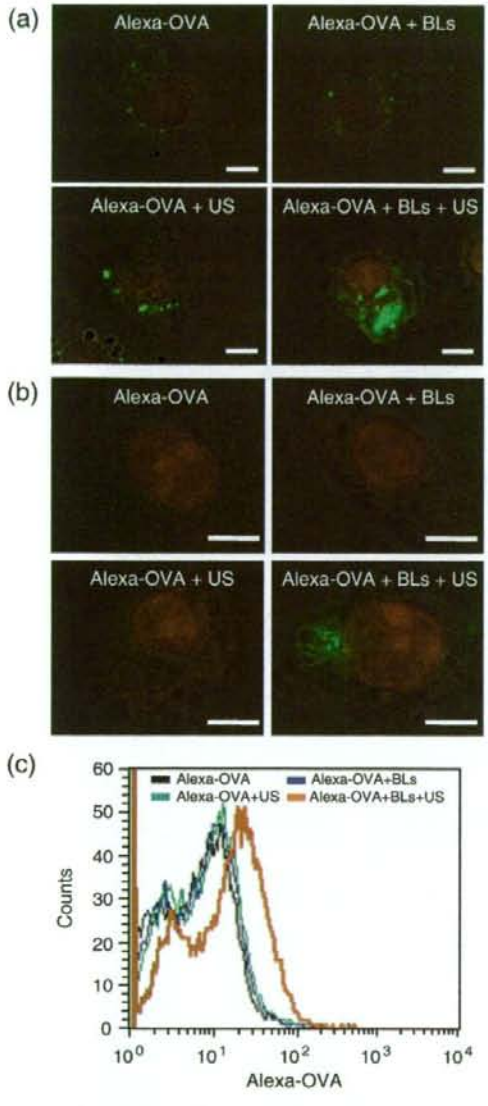

Fig. 1. Intracellular antigen delivery into DCs using BLs and US exposure. (a) Uptake of Alexa-OVA into DCs. DCs were cultured in a glass bottom dish overnight. After washing the cells, Alexa-OVA was added to the dish. Then, the DCs were exposed to US in the presence or absence of BLs and incubated for 1 h at 37 °C. The DCs were washed with PBS, fixed, and the nuclei were stained with propidium iodide. The uptake of Alexa-OVA was observed using a confocal laser microscope. (b) Intracellular delivery of Alexa-OVA into DCs using BLs and US. DCs were pretreated with OptiMEM containing 10 mM NaN_3 for 1 h at 4 °C to inhibit the endocytosis pathway. After washing the cells, Alexa-OVA was added to the DCs in OptiMEM containing10 mM NaN_3. Then, the DCs were exposed to US in the presence or absence of BLs. After US exposure, the DCs were washed with PBS containing 10 mM NaN_3, fixed, and the nuclei were stained with propidium iodide. Intracellular trafficking of Alexa-OVA in the DCs was observed using a confocal laser microscope. Scale bar shows 5 μm. (c) Flow cytometry analysis of DCs containing Alexa-OVA delivered using BLs and US. Alexa-OVA was delivered into the cell interior of the DCs during endocytosis inhibition. After washing the cells, the DCs were analyzed by flow cytometry.

inhibited. These results suggest that the combination of BLs and US exposure can be used to directly deliver antigens into the cytosol of DCs in the absence of endocytosis.

3.2. MHC class I presentation of exogenous antigen delivered into DCs by BLs and US exposure

Exogenous antigen delivered into the cytosol of DCs by BLs and US exposure is recognized as endogenous antigen by DCs and leads to the efficient presentation of peptides derived from exogenous antigens on MHC class I molecules. Thus, we examined whether antigen delivery by BLs and US exposure resulted in the efficient presentation of peptides on MHC class I molecules and the stimulation of $CD8^+$ T cells. C57BL/6-derived OVA-specific T cell hybridoma CD8-OVA1.3 was co-cultured with mouse bone marrow-derived DCs pulsed with antigen. As shown in Fig. 2, CD8-OVA1.3 cells stimulated with DCs pulsed with soluble OVA, either treated or untreated by BLs or US exposure did not secrete a significant amount of IL-2. Of note, a larger amount of IL-2 was secreted by CD8-OVA1.3 cells stimulated with DCs pulsed with OVA treated with a combination of BLs and US exposure. These data indicate that antigen delivery by BLs to DCs upon sonoporation results in the presentation of peptides derived from OVA on MHC class I molecules. In this data, the level of IL-2 secretion increased depending on OVA concentration and reached plateau in 100 μg/ml of OVA concentration. Therefore, we used this OVA concentration (100 μg/ml) in further examinations.

3.3. Cytotoxicity to DCs by the treatment of BLs and US exposure

In this antigen delivery system using BLs and US exposure, the transient pores would be provided on the membrane of DCs. Therefore, it is concerned that the DCs are injured by US exposure in the presence of BLs. To assess the cytotoxicity to DCs by the treatment of BLs and US exposure, we examined about the viability of DCs (Fig. 3). In the treatment of DC with BLs and/or US exposure, the viability of DCs treated with BLs, US exposure or BLs/US exposure was 83 ± 11%, 96 ± 5% or 87 ± 13%, respectively. This result shows that there is not serious damage to DCs even under the condition of inducing transient pores on the membrane of DCs treated with BLs and US exposure.

3.4. Induction of antigen-specific CTL response in the immunization of DCs pulsed with antigen using BLs and US exposure

To examine whether efficient peptide presentation on MHC class I molecules leads to strong induction of antigen-specific CTLs *in vivo*, we immunized C57BL/6 mice twice with bone marrow-derived DCs that had been treated with various antigen delivery techniques. Thereafter, splenocytes were isolated, and a cytotoxicity assay was

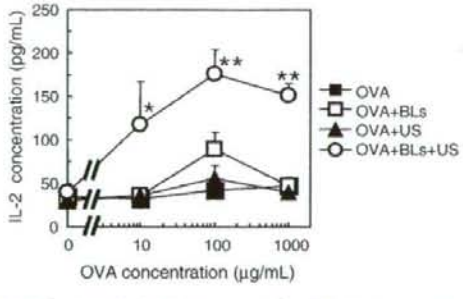

Fig. 2. MHC class I restricted OVA presentation after OVA delivery into DCs using a combination of BLs and US exposure. DCs were pulsed with OVA alone or OVA in conjunction with US exposure and/or BLs. After US exposure, the DCs were incubated for 1 h at 37 °C, then washed with PBS. After culturing for 24 h, the DCs were co-cultured with CD8-OVA1.3 cells for 20 h. The concentration of IL-2 in the supernatants was measured. Each data represents the mean ± S.D. for triplicate measurements. $^*P<0.05$ compared to the group treated with BLs or US, or without BLs and US. $^{**}P<0.01$ compared to the group treated with BLs or US, or without BLs and US.

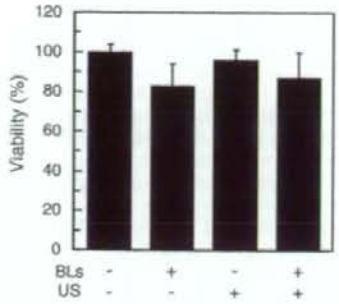

Fig. 3. Viability of DCs treated with BLs and /or US exposure. DCs were treated with BLs and/or US. After US exposure, DCs were incubated for 1 h at 37 °C, then washed with PBS. After culturing for 48 h, the viability of DCs was measured by MTT assay. Each data represents the mean ± S.D. for triplicate measurements.

performed using the syngeneic lymphoma cell line EL-4 or its OVA transfectant, E.G7-OVA. As shown in Fig. 4, immunization with DCs without OVA, DCs pulsed with OVA, or OVA combined with BLs or US exposure, induced weak cytotoxicity of splenocytes against the OVA-expressing cell line E.G7-OVA. In contrast, immunization with DCs pulsed with OVA following BL and US exposure resulted in strong cytotoxicity against the OVA-expressing cell line E.G7-OVA by splenocytes. Splenocytes from mice immunized with DCs pulsed using any method of antigen delivery did not exhibit strong cytotoxicity against the parental cell line EL-4. These data indicate that DCs pulsed with antigen using BLs and US exposure as the antigen delivery method efficiently present peptides on MHC class I molecules, which results in strong induction of antigen-specific CTLs *in vivo*.

3.5. Antitumor effects in the immunization of DCs pulsed with antigen by BLs and US exposure

Using an E.G7-OVA tumor model, we examined whether the strong induction of CTLs by antigen delivery with BLs and US exposure leads to efficient anti-tumor immune responses *in vivo*. We immunized C57BL/6 mice twice with bone marrow-derived DCs that had been pulsed using one of two methods of antigen delivery (OVA with US exposure, or OVA with BLs and US exposure). One week after the second immunization, the mice were inoculated intradermally with E.G7-OVA cells, and tumor growth was monitored. As shown in Fig. 5(a) and (b), immunization with untreated DCs weakly suppressed tumor growth. The survival rate of mice immunized with untreated DCs was slightly prolonged, suggesting that non-specific inflammatory responses induced by the injection of DCs result in weak anti-tumor immune responses. Immunization with DCs that had been pulsed with OVA using US exposure suppressed tumor growth slightly more efficiently than the control immunization. Of note, immunization with DCs that had been pulsed with OVA using BLs and US exposure completely suppressed tumor growth, with all mice in this group surviving more than 70 days after tumor inoculation. In addition, we examined the prevention of tumor growth recurrence after re-inoculation of tumor cells into mice, which had completely rejected the first injection of tumor cells (Fig. 5(c)). All mice, which were re-inoculated with E.G7-OVA cells 10 weeks after the first inoculation, completely rejected the tumor cells.

Finally, we examined whether immunization with DCs pulsed with antigen using BLs and US exposure can efficiently suppress the growth of established tumors. For this purpose, we inoculated C57BL/6 mice with E.G7-OVA, and after 9 and 12 days, when the tumors were between 100–200 mm^3, DCs were injected intradermally. As shown in Fig. 6(a), administration of untreated DCs did not provide a significant therapeutic effect. Administration of DCs pulsed with OVA using US exposure exhibited a weak therapeutic effect. Importantly, administration of DCs pulsed with OVA using BLs and US exposure exhibited stronger therapeutic effects in two of the five mice, with these two mice surviving for more than 60 days (Fig. 6(b)). These data indicate that antigen delivery into DCs with BLs and US exposure can induce significant therapeutic effects on established tumors.

4. Discussion

Subunit vaccines utilizing MHC class I-binding peptides have significant limitations that hinder their application to the general patient population (restrictions of HLA types) and that also affect their clinical effectiveness (monovalency of tumor specific antigen) in DC-based tumor immunotherapy. Utilization of tumor associated proteins as antigens may overcome this limitation, thereby enabling a broad spectrum of peptide presentation. In fact, patients treated with tumor cell lysates pulsed DCs showed better response rates compared with patients treated with peptide pulsed DCs [40]. This clinical trial suggests that tumor lysates are a good source of tumor antigens for a polyvalent antitumor vaccine. On the other hand, MHC class I molecules generally present endogenous antigens, whereas exogenous antigens for DCs are taken up by the endocytosis pathway and exogenous antigen-derived peptides are presented on MHC class II molecules [3]. In this study, we showed that by using a combination of BLs and US exposure, exogenous antigen was directly delivered into the cytosol of DCs (Fig. 1) and was presented on MHC class I molecules (Fig. 2). In addition, DCs immunized with antigen delivered by BLs and US exposure could stimulate antigen-specific CTL activation (Fig. 4) and resulted in inducing effective anti-tumor immune responses in tumor-bearing mice. (Figs. 5 and 6) Although peptide and protein delivery with sonoporation using microbubbles have been previously reported [28,29,41], the present study is the first report of effective antigen delivery into DCs by BLs using sonoporation for cancer immunotherapy.

Sonoporation and microbubbles such as Optison have been reported to be an effective gene delivery method using non-viral vectors. In addition, peptide and protein delivery with microbubbles and US exposure has been reported [28,29,41]. In the reports, Bekeredjian et al. showed the feasibility of microbubbles and US exposure for delivery of bioactive protein (luciferase, 60 kDa) into the cytosol of *in vitro* and *in vivo* cells [28,29]. Larina I.V. et al. reported that FITC-dextrans of 10–2000 kDa were delivered into human breast

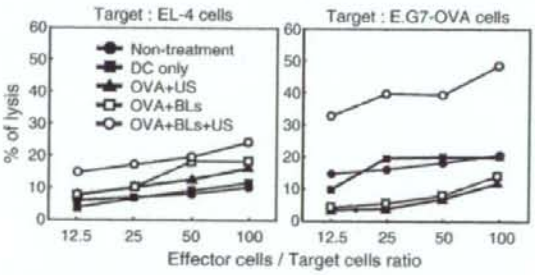

Fig. 4. Antigen specific CTL induction after immunization with DCs treated with BLs and US exposure. DCs were pulsed with OVA under each condition and cultured. After washing the cells, the DCs were intradermally injected into the backs of C57BL/6 mice. After 7 days, the mice were re-immunized. Seven days after the second immunization, splenocytes were obtained and stimulated with mitomycin C-treated E.G7-OVA cells at a ratio of 10:1 for 5 days. The stimulated splenocytes were used as effector cells for a cytotoxicity assay, using EL-4 or E.G7-OVA cells as the target in a flow cytometric assay.

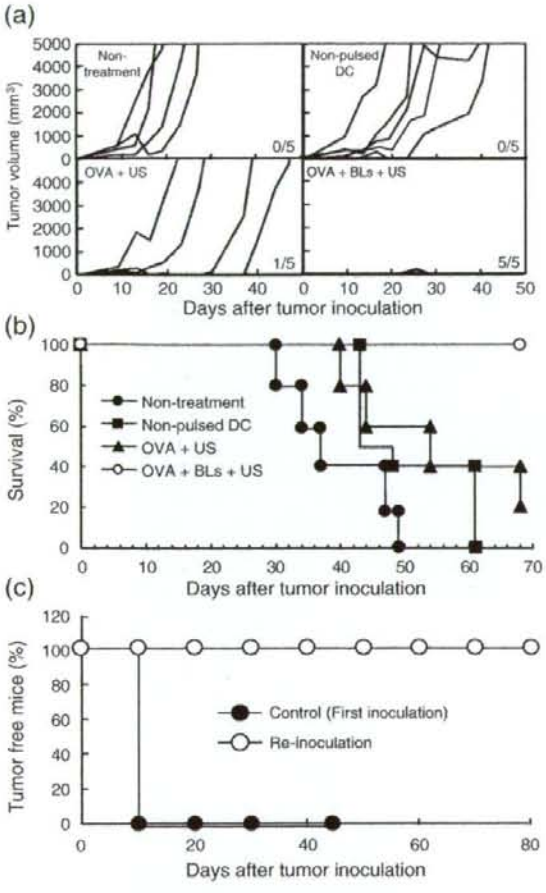

Fig. 5. Antitumor effect caused by immunization of DCs treated with antigen, BLs and US exposure. C57BL/6 mice were immunized with DCs twice. Seven days after the second immunization, E.G7-OVA cells were intradermally inoculated into the backs of the mice, and the tumor volume and survival of the mice was monitored. (a): Tumor volume of the mice after tumor inoculation. Each line indicates the tumor volume in an individual mouse. The fractional number in the lower right of each group shows the number of mice completely rejecting tumors / the number of total experimental mice. (b): Survival rate of the mice after tumor inoculation. (c): Tumor rejection efficiency after re-inoculation with tumor cells. E.G7-OVA cells were re-injected into the mice, which had rejected tumor cells following immunization with DCs treated with OVA, BLs and US in a prior immunization (a). Normal mice were used as controls to confirm the development of cancer following the first inoculation with E.G7-OVA cells. All treated groups contained five mice.

adenocarcinoma (MCF7) by the combination of Optison (conventional microbubbles) and US exposure [42]. It is believed that the delivery mechanism is due to the presence of transient pores through the cell membrane, resulting in extracellular molecules being directly delivered into the cytosol [22,43]. As shown in Fig. 1(b), antigen was directly delivered into DCs by the combination of BLs and US exposure even when the endocytosis pathway was inhibited. Therefore, it is thought that the antigen delivery mechanism induced by BLs and sonoporation is the same as that induced by microbubbles and sonoporation. In studies using microbubbles and sonoporation, pore sizes (based on the physical diameter of the component compounds) were typically between 30–100 nm, and estimates of the membrane recovery time ranged from a few seconds to a few minutes [44]. On the other hand, in studies on the aftereffects of US exposure on cell membranes, Eshet *et al.* reported that microbubbles resulted in a rougher cell surface characterized by depressions, but that the effects are reversible within 24 h following US exposure [43]. In the present study, DCs were incubated with antigen for 1 h after US exposure and increased the delivery efficiency of antigen into the cytosol of DCs. We confirmed the efficiency of MHC class I antigen presentation in DCs with/without 1 h incubation after US exposure. The efficiency following 1 h incubation was higher than that without incubation (data not shown). This result suggests that the membrane permeability of DCs increases even after US exposure. Although the mechanism behind antigen delivery by BLs is unknown, our data support a temporary increase in permeability of the plasma membrane after US exposure. Moreover, recent data from microbubble studies suggest that the resealing of US-induced pores is an energy-dependent process, with the cells exhibiting morphological features consistent with an active and vesicle-based wound-healing responses [45]. Therefore, cells treated with sonoporation are viable due to this recovery mechanism. In this study, the viability of the DCs treated with BLs and US exposure was maintained more than 85% (Fig. 3). The accumulated evidence suggests that the combination of BLs and US exposure is an unique antigen delivery system which can deliver exogenous antigens into the cytosol without serious damage to DCs.

In this study, exogenous antigens, directly delivered into the cytosol of DCs by means of BLs and US exposure, were presented on MHC class I molecules. In addition, immunization of DCs treated with antigen, BLs and US exposure effectively primed antigen-specific CTLs. On the other hand, MHC class I antigen presentation lead to low-level

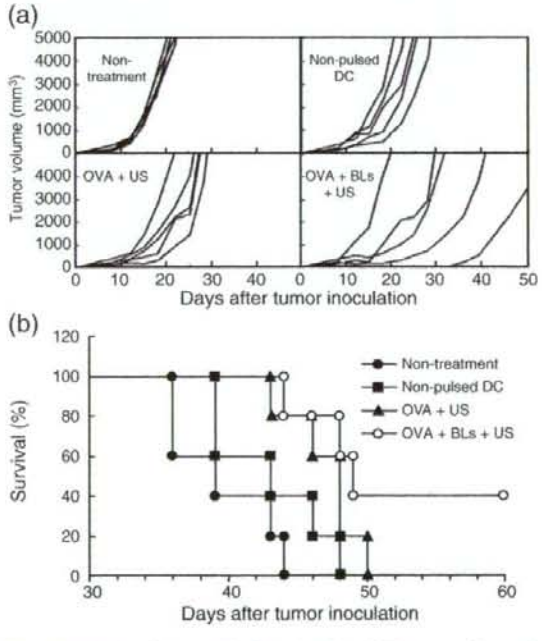

Fig. 6. Immunization of DCs treated with antigen, BLs and US exposure: therapeutic effect on tumor growth. E.G7-OVA cells were intradermally inoculated into the backs of C57BL/6 mice. On day 9, at a tumor size of 8–10 mm, OVA pulsed DCs were intradermally injected into the backs of the mice. On day 12, DCs were injected similarly. The tumor volume and survival of the mice was monitored. (a): Tumor volume of the mice after tumor inoculation. Each line indicates the tumor volume in individual mice. (b): Survival rate of the mice after tumor inoculation. All treated groups contained five mice.

antigen delivery with either BLs or US exposure. In these treated cells, antigen was mainly taken up via the endocytosis pathway. Although we have not confirmed MHC class II presentation, the antigen would presumably be presented on MHC class II molecules to DCs via the general antigen processing mechanism [10]. The exogenous antigens directly delivered into the cytosol would be processed similarly endogenously derived antigens, which are enzymatically digested into peptides, mainly by cytosolic proteases called proteasomes, and are then transported by transporters associated with antigen processing (TAP) molecules into the endoplasmic reticulum (ER). In the ER lumen, peptides bind to MHC class I molecules, which are subsequently transported via the Golgi apparatus to the cell surface [46]. Moreover, immunization of DCs treated with OVA, BLs and US exposure could prime OVA-specific CTLs. This result indicates that DCs presented with OVA-derived epitope peptides on MHC class I molecules effectively prime OVA-specific CTLs *in vivo*. We suspected that the effective priming of antigen-specific CTLs would result in the rejection of tumor cells. As shown in Fig. 5(a), all the immunized mice completely rejected the inoculated tumor cells. Tumor cells were intradermally re-injected into these mice to re-challenge their immune system and assess the preventive effects of immunization for suppressing tumor regeneration (Fig. 5(c)). Rejection following re-challenge with tumor cells suggests the induction of an antigen memory system in the host's immune system, i.e., memory T cells for the immunization antigen. Thus, this therapeutic method has potential for suppressing the regeneration and metastasis of tumors. Finally, we also assessed the therapeutic effects of this treatment towards established tumors (Fig. 6). Immunization with DCs treated with antigen, BLs and US exposure lead to significant therapeutic effects towards established tumors. Tumor cells generally secrete cytokines such as TGF-β to suppress the host's immune system. It is therefore possible that antigen delivery with BLs and US exposure could effectively induce an anti-tumor immune response even in the presence of established tumors.

In conclusion, we have developed a novel system for delivering antigens into DCs using BLs and sonoporation. Immunization of DCs using this antigen delivery system could effectively prime the anti-tumor immune system due to the induction of MHC class I TAA presentation. Therefore, BLs in conjunction with sonoporation might be a useful antigen delivery system for DC-based cancer immunotherapy. In the future, this system will be applied to various antigens containing unknown TAAs, such as crude antigens separated from surgically-removed human tumors.

Acknowledgments

The authors thank Mr. Shota Otake, Mr. Norihito Nishiie, Mr. Ken Osawa, Ms. Risa Koshima, Ms. Motoka Kawamura, Mr. Ryo Tanakadate, Mr. Kunihiko Matsuo and Mr. Yasuyuki Shiono (Teikyo University) for their technical assistance, and Mr. Yasuhiko Hayakawa, Mr. Takahiro Yamauchi and Mr. Kosho Suzuki (Nepa Gene Co., Ltd.) for their technical advice regarding US exposure. This study was supported by the Program for Promotion of Fundamental Studies in Health Sciences of the National Institute of Biomedical Innovation (NIBIO). Tetsuya Kodama acknowledges the Grant for Research on Nanotechnical Medical, the Ministry of Health, Labour and Welfare of Japan (H19-nano-010).

References

[1] F.O. Nestle, A. Farkas, C. Conrad, Dendritic-cell-based therapeutic vaccination against cancer, Curr. Opin. Immunol. 17 (2005) 163–169.
[2] J. Copier, A. Dalgleish, Overview of tumor cell-based vaccines, Int. Rev. Immunol. 25 (2006) 297–319.
[3] R.N. Germain, MHC-dependent antigen processing and peptide presentation: providing ligands for T lymphocyte activation, Cell 76 (1994) 287–299.
[4] P. Elamanchili, M. Diwan, M. Cao, J. Samuel, Characterization of poly(D,L-lactic-co-glycolic acid) based nanoparticulate system for enhanced delivery of antigens to dendritic cells, Vaccine 22 (2004) 2406–2412.
[5] T. Yoshikawa, N. Okada, A. Oda, K. Matsuo, K. Matsuo, Y. Mukai, Y. Yoshioka, T. Akagi, M. Akashi, S. Nakagawa, Development of amphiphilic gamma-PGA-nanoparticle based tumor vaccine: potential of the nanoparticulate cytosolic protein delivery carrier, Biochem. Biophys. Res. Commun. 366 (2008) 408–413.
[6] P. Machy, K. Serre, L. Leserman, Class I-restricted presentation of exogenous antigen acquired by Fcgamma receptor-mediated endocytosis is regulated in dendritic cells, Eur. J. Immunol. 30 (2000) 848–857.
[7] N. Okada, T. Saito, K. Mori, Y. Masunaga, Y. Fujii, J. Fujita, K. Fujimoto, T. Nakanishi, K. Tanaka, S. Nakagawa, T. Mayumi, T. Fujita, A. Yamamoto, Effects of lipofectin-antigen complexes on major histocompatibility complex class I-restricted antigen presentation pathway in murine dendritic cells and on dendritic cell maturation, Biochim. Biophys. Acta 1527 (2001) 97–101.
[8] L. Wang, H. Ikeda, Y. Ikuta, M. Schmitt, Y. Miyahara, Y. Takahashi, X. Gu, Y. Nagata, Y. Sasaki, K. Akiyoshi, J. Sunamoto, H. Nakamura, K. Kuribayashi, H. Shiku, Bone marrow-derived dendritic cells incorporate and process hydrophobized polysaccharide/oncoprotein complex as antigen presenting cells, Int. J. Oncol. 14 (1999) 695–701.
[9] K. Kawamura, N. Kadowaki, R. Suzuki, S. Udagawa, S. Kasaoka, N. Utoguchi, T. Kitawaki, N. Sugimoto, N. Okada, K. Maruyama, T. Uchiyama, Dendritic cells that endocytosed antigen-containing IgG-liposomes elicit effective antitumor immunity, J. Immunother. 29 (2006) 165–174.
[10] K.W. Kim, S.H. Kim, J.H. Jang, E.Y. Lee, S.W. Park, J.H. Um, Y.J. Lee, C.H. Lee, S. Yoon, S.Y. Seo, M.H. Jeong, S.T. Lee, B.S. Chung, C.D. Kang, Dendritic cells loaded with exogenous antigen by electroporation can enhance MHC class I-mediated antitumor immunity, Cancer Immunol. Immunother. 53 (2004) 315–322.
[11] J.M. Weiss, C. Allen, R. Shivakumar, S. Feller, L.H. Li, L.N. Liu, Efficient responses in a murine renal tumor model by electroloading dendritic cells with whole-tumor lysate, J. Immunother. 28 (2005) 542–550.
[12] M. Fechheimer, J.F. Boylan, S. Parker, J.E. Sisken, G.L. Patel, S.G. Zimmer, Transfection of mammalian cells with plasmid DNA by scrape loading and sonication loading, Proc. Natl. Acad. Sci. U. S. A. 84 (1987) 8463–8467.
[13] M.W. Miller, D.L. Miller, A.A. Brayman, A review of in vitro bioeffects of inertial ultrasonic cavitation from a mechanistic perspective, Ultrasound Med. Biol. 22 (1996) 1131–1154.
[14] M. Joersbo, J. Brunstedt, Protein synthesis stimulated in sonicated sugar beet cells and protoplasts, Ultrasound Med. Biol. 16 (1990) 719–724.
[15] D.L. Miller, S.V. Pislaru, J.E. Greenleaf, Sonoporation: mechanical DNA delivery by ultrasonic cavitation, Somat. Cell Mol. Genet. 27 (2002) 115–134.
[16] H.R. Guzman, A.J. McNamara, D.X. Nguyen, M.R. Prausnitz, Bioeffects caused by changes in acoustic cavitation bubble density and cell concentration: a unified explanation based on cell-to-bubble ratio and blast radius, Ultrasound Med. Biol. 29 (2003) 1211–1222.
[17] W. Wei, B. Zheng-zhong, W. Yong-jie, Z. Qing-wu, M. Ya-lin, Bioeffects of low-frequency ultrasonic gene delivery and safety on cell membrane permeability control, J. Ultrasound Med. 23 (2004) 1569–1582.
[18] H.J. Kim, J.F. Greenleaf, R.R. Kinnick, J.T. Bronk, M.E. Bolander, Ultrasound-mediated transfection of mammalian cells, Hum. Gene Ther. 7 (1996) 1339–1346.
[19] D.B. Tata, F. Dunn, D.J. Tindall, Selective clinical ultrasound signals mediate differential gene transfer and expression in two human prostate cancer cell lines: LnCap and PC-3, Biochem. Biophys. Res. Commun. 234 (1997) 64–67.
[20] M. Duvshani-Eshet, M. Machluf, Therapeutic ultrasound optimization for gene delivery: a key factor achieving nuclear DNA localization, J. Control. Release 108 (2005) 513–528.
[21] W.J. Greenleaf, M.E. Bolander, G. Sarkar, M.B. Goldring, J.F. Greenleaf, Artificial cavitation nuclei significantly enhance acoustically induced cell transfection, Ultrasound Med. Biol. 24 (1998) 587–595.
[22] Y. Taniyama, K. Tachibana, K. Hiraoka, M. Aoki, S. Yamamoto, K. Matsumoto, T. Nakamura, T. Ogihara, Y. Kaneda, R. Morishita, Development of safe and efficient novel nonviral gene transfer using ultrasound: enhancement of transfection efficiency of naked plasmid DNA in skeletal muscle, Gene Ther. 9 (2002) 372–380.
[23] S. Chen, J.H. Ding, R. Bekeredjian, B.Z. Yang, R.V. Shohet, S.A. Johnston, H.E. Hohmeier, C.B. Newgard, P.A. Grayburn, Efficient gene delivery to pancreatic islets with ultrasonic microbubble destruction technology, Proc. Natl. Acad. Sci. U. S. A. 103 (2006) 8469–8474.
[24] A. Aoi, Y. Watanabe, S. Mori, M. Takahashi, G. Vassaux, T. Kodama, Herpes simplex virus thymidine kinase-mediated suicide gene therapy using nano/microbubbles and ultrasound, Ultrasound Med. Biol. 34 (2008) 425–434.
[25] Z.P. Shen, A.A. Brayman, L. Chen, C.H. Miao, Ultrasound with microbubbles enhances gene expression of plasmid DNA in the liver via intraportal delivery, Gene Ther. (2008).
[26] S. Sonoda, K. Tachibana, E. Uchino, A. Okubo, M. Yamamoto, K. Sakoda, T. Hisatomi, K.H. Sonoda, Y. Negishi, Y. Izumi, S. Takao, T. Sakamoto, Gene transfer to corneal epithelium and keratocytes mediated by ultrasound with microbubbles, Investig. Ophthalmol. Vis. Sci. 47 (2006) 558–564.
[27] K. Iwanaga, K. Tominaga, K. Yamamoto, M. Habu, H. Maeda, S. Akifusa, T. Tsujisawa, T. Okinaga, J. Fukuda, T. Nishihara, Local delivery system of cytotoxic agents to tumors by focused sonoporation, Cancer Gene Ther. 14 (2007) 354–363.
[28] R. Bekeredjian, S. Chen, P.A. Grayburn, R.V. Shohet, Augmentation of cardiac protein delivery using ultrasound targeted microbubble destruction, Ultrasound Med. Biol. 31 (2005) 687–691.
[29] R. Bekeredjian, H.F. Kuecherer, R.D. Kroll, H.A. Katus, S.E. Hardt, Ultrasound-targeted microbubble destruction augments protein delivery into testes, Urology 69 (2007) 386–389.
[30] T. Yamashita, S. Sonoda, R. Suzuki, N. Arimura, K. Tachibana, K. Maruyama, T. Sakamoto, A novel bubble liposome and ultrasound-mediated gene transfer to ocular surface: RC-1 cells in vitro and conjunctiva in vivo, Exp. Eye Res. 85 (2007) 741–748.

[31] R. Suzuki, T. Takizawa, Y. Negishi, K. Hagisawa, K. Tanaka, K. Sawamura, N. Utoguchi, T. Nishioka, K. Maruyama, Gene delivery by combination of novel liposomal bubbles with perfluoropropane and ultrasound, J. Control. Release 117 (2007) 130–136.
[32] R. Suzuki, T. Takizawa, Y. Negishi, N. Utoguchi, K. Maruyama, Effective gene delivery with novel liposomal bubbles and ultrasonic destruction technology, Int. J. Pharm. 354 (2008) 49–55.
[33] R. Suzuki, T. Takizawa, Y. Negishi, N. Utoguchi, K. Sawamura, K. Tanaka, E. Namai, Y. Oda, Y. Matsumura, K. Maruyama, Tumor specific ultrasound enhanced gene transfer in vivo with novel liposomal bubbles, J. Control. Release 125 (2008) 137–144.
[34] R. Suzuki, T. Takizawa, Y. Negishi, N. Utoguchi, K. Maruyama, Effective gene delivery with liposomal bubbles and ultrasound as novel non-viral system, J. Drug Target. 15 (2007) 531–537.
[35] J.D. Pfeifer, M.J. Wick, R.L. Roberts, K. Findlay, S.J. Normark, C.V. Harding, Phagocytic processing of bacterial antigens for class I MHC presentation to T cells, Nature 361 (1993) 359–362.
[36] K. Inaba, M. Inaba, M. Deguchi, K. Hagi, R. Yasumizu, S. Ikehara, S. Muramatsu, R.M. Steinman, Granulocytes, macrophages, and dendritic cells arise from a common major histocompatibility complex class II-negative progenitor in mouse bone marrow, Proc. Natl. Acad. Sci. U. S. A. 90 (1993) 3038–3042.
[37] D.P. Guo, X.Y. Li, P. Sun, Y.B. Tang, X.Y. Chen, Q. Chen, L.M. Fan, B. Zang, L.Z. Shao, X.R. Li, Ultrasound-targeted microbubble destruction improves the low density lipoprotein receptor gene expression in HepG2 cells, Biochem. Biophys. Res. Commun. 343 (2006) 470–474.
[38] T. Mosmann, Rapid colorimetric assay for cellular growth and survival: application to proliferation and cytotoxicity assays, J. Immunol. Methods 65 (1983) 55–63.
[39] S.E. Slezak, P.K. Horan, Cell-mediated cytotoxicity. A highly sensitive and informative flow cytometric assay, J. Immunol. Methods 117 (1989) 205–214.
[40] G. Reinhard, A. Marten, S.M. Kiske, F. Feil, T. Bieber, I.G. Schmidt-Wolf, Generation of dendritic cell-based vaccines for cancer therapy, Br. J. Cancer 86 (2002) 1529–1533.
[41] M. Kinoshita, K. Hynynen, Intracellular delivery of Bak BH3 peptide by microbubble-enhanced ultrasound, Pharm. Res. 22 (2005) 716–720.
[42] I.V. Larina, B.M. Evers, R.O. Esenaliev, Optimal drug and gene delivery in cancer cells by ultrasound-induced cavitation, Anticancer Res. 25 (2005) 149–156.
[43] M. Duvshani-Eshet, D. Adam, M. Machluf, The effects of albumin-coated microbubbles in DNA delivery mediated by therapeutic ultrasound, J. Control. Release 112 (2006) 156–166.
[44] C.M. Newman, T. Bettinger, Gene therapy progress and prospects: ultrasound for gene transfer, Gene Ther. 14 (2007) 465–475.
[45] R.K. Schlicher, H. Radhakrishna, T.P. Tolentino, R.P. Apkarian, V. Zarnitsyn, M.R. Prausnitz, Mechanism of intracellular delivery by acoustic cavitation, Ultrasound Med. Biol. 32 (2006) 915–924.
[46] P.M. Kloetzel, Antigen processing by the proteasome, Nat. Rev. Mol. Cell. Biol. 2 (2001) 179–187.

Journal of Controlled Release 132 (2008) 124–130

Contents lists available at ScienceDirect

Journal of Controlled Release

journal homepage: www.elsevier.com/locate/jconrel

Delivery of siRNA into the cytoplasm by liposomal bubbles and ultrasound

Yoichi Negishi [a,*,1], Yoko Endo [a,1], Tetsuya Fukuyama [a], Ryo Suzuki [b], Tomoko Takizawa [b], Daiki Omata [a], Kazuo Maruyama [b], Yukihiko Aramaki [a]

[a] Department of Drug and Gene Delivery System, School of Pharmacy, Tokyo University of Pharmacy and Life Sciences, Hachioji, Tokyo, Japan
[b] Department of Biopharmaceutics, School of Pharmaceutical Sciences, Teikyo University, Sagamihara, Kanagawa, Japan

ARTICLE INFO

Article history:
Received 12 April 2008
Accepted 27 August 2008
Available online 7 September 2008

Keywords:
siRNA delivery
Ultrasound
Bubble liposomes

ABSTRACT

Small interfering RNA (siRNA) is expected to be a novel therapeutic tool, however, its utilization has been limited by inefficient delivery systems. Recently, we have developed novel polyethyleneglycol modified liposomes (Bubble liposomes; BL) entrapping an ultrasound (US) imaging gas, which can work as a gene delivery tool with US exposure. In this study, we investigated whether the BL were suitable for the delivery of siRNA. BL efficiently delivered siRNA with only 10 s of exposure to US *in vitro*. Specific gene silencing effects could be achieved well even in the presence of serum or with the disruption of endocytosis. We suggest that siRNA is directly introduced into the cytoplasm by the BL and US and the mechanism enables effective transfection within a short time and in the presence of high serum. Transfection of siRNA into the tibialis muscles with BL and US was also performed. The gene-silencing effect could be sustained for more than 3 weeks. Thus, BL could be a useful siRNA delivery tool *in vitro* and *in vivo*.

1. Introduction

RNA interference (RNAi) has potential in the development of new treatments for disease, including malignant, infectious and autoimmune diseases. In order to achieve efficient gene silencing, it is important that the siRNA is introduced into the cytoplasm of the target cell. Diverse approaches have been attempted to develop efficient siRNA delivery methods [1–7]. However, technologies that enable the tissue-targeted delivery of siRNA using non-viral vectors need improvements.

One novel approach to the administration of a drug or gene is the method of US-enhanced delivery. US-enhanced delivery often exploits the cavitation bubbles produced by the pressure oscillations of US. Furthermore, US pressures above a certain threshold can cause oscillating bubbles to undergo a violent collapse known as inertial cavitation. Inertial cavitation is believed to cause transient disruptions in cell membranes, enabling the transport of extracellular molecules into viable cells [8–12]. Microbubbles, which are contrast agents for medical US imaging, improve gene transfection efficiency after US-induced cavitation [13–19]. However, microbubbles have problems with size, stability, and targeting function.

Liposomes, useful carriers of drugs, antigens, and genes, can be easily prepared in a variety of sizes and modified to add a targeting function [20–24]. Therefore, we considered that polyethyleneglycol-modified liposomes containing the US imaging gas could be novel gene delivery carriers. Then we reported that "Bubble liposomes (BL)" were feasible for delivering genes *in vitro* and *in vivo* [25–27]. In this study, we assessed whether BL accompanied by US are also useful for the delivery of siRNA *in vitro* and *in vivo*. We further investigated the mechanism of the transfection with BL and US to clarify the involvement of the endosomal pathway compared to other transfection methods thought to carry nucleic acids into cells via endocytosis.

2. Materials and methods

2.1. Cell lines and cultures

COS-7, NIH3T3 and C2C12 cells were cultured in Dulbecco's modified Eagle's medium (DMEM; Kohjin Bio Co. Ltd., Tokyo, Japan) supplemented with 10% heat-inactivated fetal bovine serum (FBS; Equitech Bio Inc., Kerrville, TX), 100 units/ml penicillin and 100 μg/ml streptomycin in a humidified atmosphere containing 5% CO_2 at 37 °C.

2.2. Preparation of liposomes and BL

Liposomes composed of 1,2-dipalmitoyl-*sn*-glycero-phosphatidylcholine (DPPC) (NOF Corporation, Tokyo, Japan) and 1,2-distearoylphosphatidylethanolamine-methoxy-polyethyleneglycol (DSPE-PEG2000-OMe) (NOF Corporation, Tokyo, Japan) (6 mol%) were prepared by a reverse phase evaporation method. In brief, all reagents were dissolved in 1:1 (v/v) chloroform/diisopropylether. Phosphate-buffered saline was added to the lipid solution and the mixture was sonicated and evaporated at 47 °C. The organic solvent was completely removed, and the size of the liposomes was adjusted to less than 200 nm

* Corresponding author. Tel./fax: +81 42 676 3183.
E-mail address: negishi@ps.toyaku.ac.jp (Y. Negishi).
[1] The first two authors contributed equally to this work.

0168-3659/$ – see front matter © 2008 Elsevier B.V. All rights reserved.
doi:10.1016/j.jconrel.2008.08.019

using extruding equipment and sizing filter (pore size: 200 nm) (Nuclepore Track-Etch Membrane, Whatman plc, UK). After the sizing, the liposomes were passed through a 0.45-μm pore size filter (Syringe filter, ASAHI TECHNO GLASS Co., Chiba, Japan) to sterilize them. The lipid concentration was measured with Phospholipid C test Wako (Wako Pure Chemical Industries, Ltd., Osaka, Japan). BL were prepared from liposomes and perfluoropropane gas (Takachiho Chemical Ind. Co. Ltd., Tokyo, Japan). First, 5-mL sterilized vials containing 2 mL of liposome suspension (lipid concentration: 1 mg/mL) were filled with perfluoropropane gas, capped, and then pressured with 7.5 mL of perfluoropropane gas. The vial was placed in a bath-type sonicator (42 kHz, 100 W) (BRANSONIC 2510J-DTH, Branson Ultrasonics Co., Danbury, CT) for 5 min to form BL.

2.3. Plasmid DNA and siRNA

The plasmid pCMV-GL3 derived from pGL3-basic (Promega, Madison, WI) is an expression vector encoding the firefly luciferase gene under the control of a cytomegalovirus promoter. The plasmid pEGFP-N3 (Clontech Laboratories, Inc., Mountain View, CA) is an expression vector encoding enhanced green fluorescein protein under the control of a cytomegalovirus promoter. pDsRed-N1 (Clontech Laboratories, Inc., Mountain View, CA) is an expression vector encoding red fluorescein protein under the control of a cytomegalovirus promoter. siRNA targeting luciferase (Luciferase GL3 siRNA; siGL3), siRNA targeting EGFP (GFP-22 siRNA; siGFP), and a non-targeting siRNA (Control (nonsil.) siRNA; siCont) were purchased from QIAGEN K.K. (Tokyo, Japan). The sequences are siGL3: *5′-CUUACGCUGAGUACUUCGAdTdT-3′* and *5′-UCGAAGUACUCAGCGUAAGdTdT-3′*, siGFP: *5′-GCAAGCUGACCCUGAAGUUCAU-3′* and *5′-GAACUUCAGGGUCAGCUUGCCG-3′*, siCont: *5′-UUCUCCGAACGUGUCACGUdTdT-3′* and *5′-ACGUGACACGUUCGGAGAAdTdT-3′*. Non-targeting fluorescein-labeled siRNA (BLOK-iT Fluorescent Oligo) was purchased from Invitrogen Japan K.K. (Tokyo, Japan). BLOCK-iT was used to determine intracellular distribution.

2.4. Transfection of pDNA and siRNA into cells using BL

The day before transfection, cells (3×10^4) were seeded in the wells of a 48-well plate (ASAHI TECHNOGLASS CO., Chiba, Japan). Five micrograms of pDNA, siRNA and 60 μg of BL were mixed together with culture medium containing 10% FBS and added to the cells. The cells were immediately exposed to US (frequency, 2 MHz; duty, 50%; burst rate, 2.0 Hz; intensity 2.5 W/cm^2) for 10 s through a 6-mm diameter probe placed in the well. A Sonopore 3000 (NEPA GENE, CO., LTD., Chiba, Japan) was used to generate the US. The cells were washed twice with culture medium and cultured for two days.

2.5. Transfection of pDNA and siRNA with Lipofectamine 2000

The day before transfection, COS-7 cells (4×10^4) were seeded in the wells of a 48-well plate (ASAHI TECHNOGLASS CO., Chiba, Japan). Then, 0.25 μg of pDNA and siRNA (final concentration, 25 nM) were diluted into Opti-MEM (GIBCO). Next, 1.25 μg of Lipofectamine 2000 (LF2000) (Invitrogen Japan K.K., Tokyo, Japan) was diluted into Opti-MEM. These solutions were mixed and added to the cells. After 4 and 24 h, the cells were washed with PBS and cultured for two days. The experiments were performed according to the manufacturers' instructions.

2.6. Localization of FITC-labeled siRNA after transfection with BL

Immediately after transfection of the FITC-labeled siRNA (200 nM) with BL and US, the cells were fixed with 4% Paraformaldehyde Phosphate Buffer and permeabilized with 0.2% saponin/0.2% BSA-PBS. The cells transfected with LF2000 were fixed and permeabilized 30 min after the transfection. To enhance the fluorescence of intercellular siRNA up to the detectable level, the fixed cells were treated with a signal amplification kit (Alexa Fluor 488 Signal-Amplification Kit Fluorescein- and Oregon Green Dye-Conjugated Probes, Invitrogen Japan K.K., Tokyo, Japan) following the manufacturer's instructions. The cells were mounted in VECTASHIELD Hard•Set Mounting Medium (Vector Laboratories, Burlingame, CA) with the

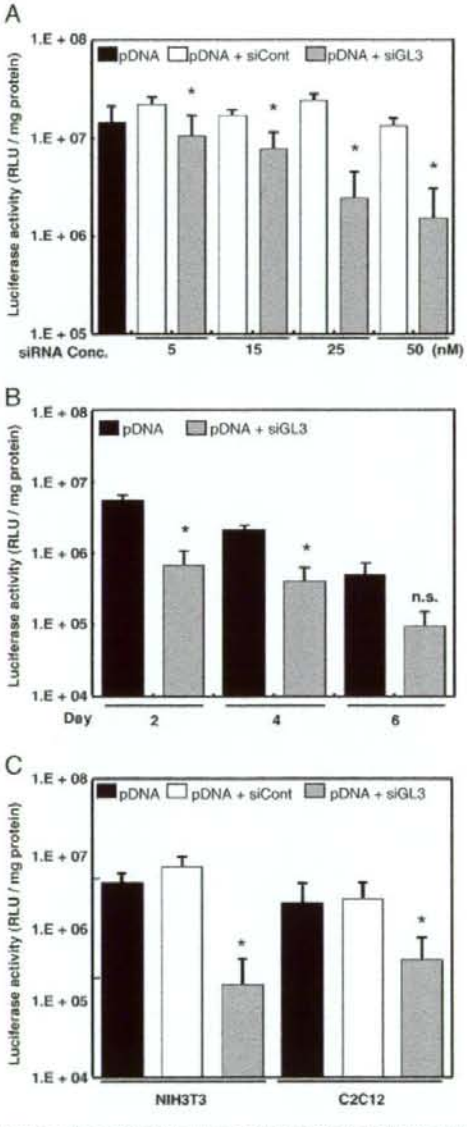

Fig. 1. Down-regulation of luciferase expression by siRNA with BL and US and cell viability after exposure to US and BL. pDNA: the group transfected with pCMV-GL3 only, pDNA + siCont; the group transfected with pCMV-GL3 and non-targeting siRNA (siCont), pDNA + siGL3; the group transfected with pCMV-GL3 and siRNA targeting luciferase (siGL3). (A) Luciferase expression in COS-7 cells transfected with pDNA and siRNA (5–50 nM) using BL and US at 2 days post-transfection. * indicates P value <0.05 compared with negative control. (B) Luciferase expression in COS-7 cells transfected with pDNA and siRNA (25 nM) using BL and US at 2, 4, and 6 days post-transfection. * indicates P value <0.05 compared with pDNA alone. (C) Luciferase expression in NIH3T3 and C2C12 cells transfected with pDNA and siRNA (25 nM) using BL and US at 2 days post-transfection. * indicates P value <0.05 compared with negative control. All data represent the mean ± S.D. ($n=4$).

coverslip cell-side down on top of a drop of the mounting medium. The samples were analyzed by confocal laser microscopy.

2.7. In vivo gene delivery into the tibialis muscle of mice with BL and US

Plasmid DNA (pCMV-GL3; 5 μg) and siRNA (3 μg) with the BL (30 μg) suspension were injected into the tibialis muscle of ICR mice (5 weeks old, male) using a 30-gauge needle (NIPRO CO., Osaka, Japan). Immediately after the injection, US (frequency, 2 MHz, duty, 50%; burst rate, 2.0 Hz; intensity, 2.5 W/cm^2; time, 60 s) was applied transdermally downstream of the injection site through a 6-mm diameter probe. Several days after the injection, the mice were sacrificed and the tibialis muscle in the US-exposed area was collected.

2.8. In vivo gene delivery into the skin and kidney of mice with BL and US

Plasmid DNA (pCMV-GL3; 5 μg) and siRNA (3 μg) with the BL (30 μg) suspension were injected into the dorsal skin of ICR mice (5 weeks old, male) by intradermal injection. The kidney was exposed and plasmid DNA (pCMV-GL3; 5 μg) and siRNA (3 μg) with the BL (30 μg) suspension were injected into the kidney of ICR mice (5 weeks old, male) by intra-renal-parenchymal injection. Immediately after the injection, US was applied to each injection site. Three days after the exposure, the mice were sacrificed and each tissue in the US-exposed area was collected.

2.9. In vivo gene delivery into the tibialis muscle of mice with electroporation

Plasmid DNAs (pEGFP-N3; 2.5 μg, pDsRed-N1; 2.5 μg) were injected into the tibialis muscle of ICR mice (5 weeks old, male) and electroporated at 140 v/cm, 50 ms (Electroporator CUY21 EDIT, NEPA GENE, CO., LTD., Chiba, Japan). After 1 day, siRNA (3 μg) was transfected with BL (30 μg) and US as described above. Three days after the US exposure, the mice were sacrificed and the tibialis muscle in the exposed area was collected.

2.10. Measurement of luciferase and EGFP expression

Cell lysate and tissue homogenates were prepared with a lysis buffer (0.1 M Tris–HCl (pH 7.8), 0.1% Triton X-100, and 2 mM EDTA). Luciferase activity was measured using a luciferase assay system (Promega, Madison, WI) and a luminometer (LB96V, Belthold Japan Co. Ltd., Tokyo, Japan). The activity is indicated as relative light units (RLU) per mg protein. For analyzing EGFP expression, the treated muscle was fixed with 2% paraformaldehyde and dehydrated in a sucrose solution. The specimens were embedded in OCT compound and immediately frozen at −80 °C. Serial sections 8 μm thick were cut by cryostat and observed with a fluorescence microscope (Axiovert 200 M, Carl Zeiss).

2.11. Experiments in vivo studies

Animal use and relevant experimental procedures were approved by the Tokyo University of Pharmacy and Life Science Committee on the Care and Use of Laboratory Animals.

2.12. Statistical analyses

All data are shown as the mean±S.D. (n=4 or 6). Data were considered significant when $P<0.05$. The t-test was used to calculate statistical significance.

3. Results

3.1. Down-regulation of luciferase expression by siRNA with BL in cultured cells

To investigate the gene silencing effects of siRNA transfected with BL and US, cells were co-transfected with pDNA encoding firefly luciferase (pCMV-GL3) and a non-targeting control or luciferase-targeting siRNA (siCont or siGL3) in the concentration range of 5–50 nM (Fig. 1A). As a result, about 90% of luciferase expression was blocked by adding more than 25 nM siRNA. We also examined the duration of this down-regulation (Fig. 1B). Although the level of expression gradually decreased, the gene silencing effects in the siGL3-treated group persisted for 4 days after the transfection. Although there appeared to be a difference at day 6, this difference was not statistically significant. The cytotoxicity of BL and US was also examined with the MTT assay and cell viability was about 90% even when the transfection was performed with 200 nM siRNA (data not shown). We further attempted the transfections of siRNA into other cell lines, like NIH3T3 and C2C12 cells. The data show that the luciferase activity was also blocked by siRNA in these two cell lines (Fig. 1C). These results suggest that BL accompanied by US is potentially useful for siRNA delivery in many cell types.

3.2. Effects of high serum on down-regulation of luciferase expression by siRNA transfected with BL and US

The transfection of siRNA should be effective in the presence of serum for clinical use. Therefore, we examined the effects of serum on the gene silencing effects of siRNA transfected with BL and US and compared them to the effects obtained with LF2000. As shown in Fig. 2, the expression of luciferase was down-regulated up to more than 90% by both transfection methods in the absence of serum. LF2000 was much more effective than BL as a tool for the delivery of pDNA and siRNA. However, the effects obtained with LF2000 were markedly decreased in a serum dose-dependent manner. This result may be due to the interference in LF2000 by serum proteins as shown in previous reports [28,29]. By contrast, the transfection with BL and US resulted in gene silencing effects with a significant difference between the siGL3-treated group and untreated group even in the presence of 50% serum. The silencing effects were slightly decreased, which was probably due to a difference in stability between pDNA and siRNA. These results suggest that the transfection with BL and US is effective in the presence of serum. The probable transfection mechanism is likely the delivery of siRNA directly into the cytoplasm within a fairly short time.

3.3. Mechanism of transfection with BL and US

To examine the involvement of endocytosis in the process, cells were pretreated for 30 min and cultured after transfection for 4 h in the presence of 50 nM chloroquine which is recognized as an endosomolytic agent (Fig. 3A). The luciferase expression and down-regulation of the

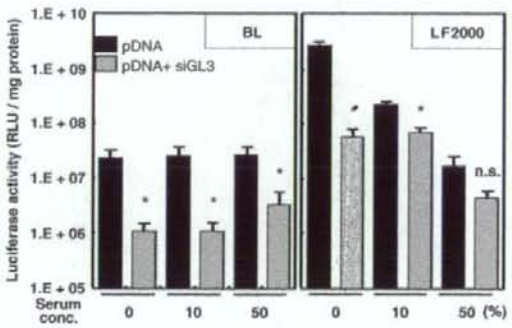

Fig. 2. Effects of high serum on down-regulation of luciferase expression by siRNA with BL and US or LF2000. pDNA; the group transfected with pCMV-GL3 only, pDNA+siGL3; the group transfected with pCMV-GL3 and siGL3. Luciferase expression in COS-7 cells transfected with pDNA and siRNA (25 nM) using BL and US or LF2000 at 2 days post-transfection in the presence of 0, 10, and 50% fetal bovine serum. * indicates P value <0.05 compared with pDNA alone. All data represent the mean±S.D. (n=4).

expression by siRNA were unaffected by the chloroquine treatment. We also investigated the effect of incubation temperature on the gene expression and down-regulation (Fig. 3B). Cells were preincubated for 30 min at 37 °C or 4 °C and co-transfected with pDNA and siRNA using BL and US. This was followed by an additional 1 h at 37 °C or 4 °C. As shown in Fig. 3B, the luciferase expression and down-regulation of the expression by siRNA were unaffected by the incubation temperature. We further evaluated the intracellular localization of siRNA transfected with BL or LF2000 by confocal microscopy (Fig. 3C). There was a significant cytoplasmic distribution of siRNA using either method. However, there was a difference in the pattern of distribution. In the case of transfection with LF2000, the fluorescence was distributed in a punctate pattern. In contrast, it was homogeneously distributed in the case of transfection with BL and US. These results suggest that the transfection with BL and US did not involve endocytosis, but the siRNA was directly introduced into the cytoplasm.

3.4. Down-regulation of luciferase expression by siRNA with BL and US in vivo

To evaluate the ability of BL to deliver siRNA *in vivo*, we attempted to co-deliver pDNA and siRNA into the tibialis muscle. As shown in Fig. 4A,

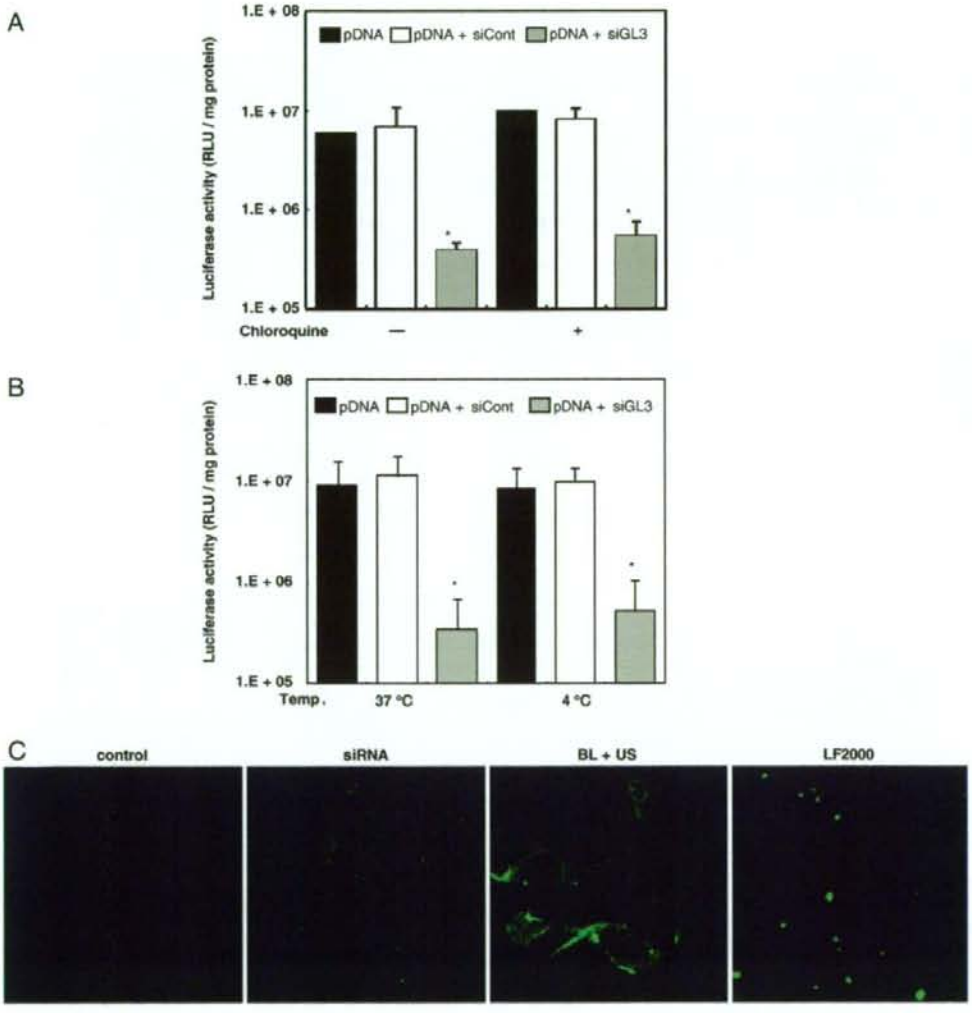

Fig. 3. The involvement of endocytosis in the process of transfection with BL. (A, B) pDNA; the group transfected with pCMV-GL3 only, pDNA+siCont; the group transfected with pCMV-GL3 and siCont, pDNA+siGL3; the group transfected with pCMV-GL3 and siGL3. (A) Luciferase expression in COS-7 cells transfected with pDNA and siRNA (25 nM) using BL and US at 2 days post-transfection with or without chloroquine (50 nM). Data represent the mean ± S.D. (n=4). * indicates P value <0.05 compared with negative control. (B) Luciferase expression in COS-7 cells transfected with pDNA and siRNA (25 nM) using BL and US and incubated at 37 °C or 4 °C for 30 min before transfection and for 1 h after transfection at 2 days post-transfection. Data represent the mean ± S.D. (n=4). * indicates P value <0.05 compared with negative control. (C) Localization of siRNA after transfection. cont; the untreated group, siRNA; the group only given FITC-siRNA, BL+US; the group transfected with FITC-siRNA using BL and US, LF2000; the group transfected with FITC-siRNA using LF2000. Confocal microscopy was used to visualize the cellular uptake and translocation of FITC-labeled siRNA (200 nM). Shown are fluorescence microscopic images of cross sections.

with the combination of BL and US, about 95% of luciferase expression was blocked by siRNA. Furthermore, the silencing effect was observed for 7 days (Fig. 4B). Although there appeared to be a difference after 7 days, this difference was not statistically significant. We further attempted the transfection to skin and kidney with BL and US. As shown in Fig. 4C, the luciferase expression had a tendency to be blocked in the skin. However, in kidney, the down-regulation was not observed and the luciferase expression was even observed in the group transfected with pCMV-GL3 only. To evaluate the silencing effects of siRNA transfected with BL and US on stably expressed genes, the day before transfection of the siRNA, we attempted to introduce pEGFP and pDsRed into tibialis muscle by electroporation which is known to be effective for gene transfection into muscle. Down-regulation of EGFP expression was observed in only the focused area of US exposure, while DsRed expression showed no change (Fig. 5). From these results, BL could be also a useful tool *in vivo*.

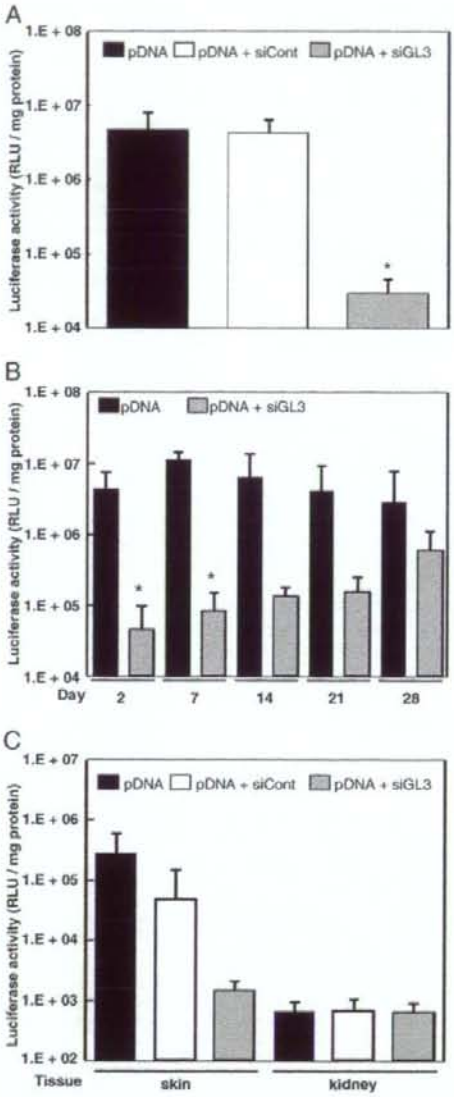

Fig. 4. Down-regulation of luciferase expression by siRNA with BL and US *in vivo*. pDNA; the group transfected with pCMV-GL3 only, pDNA+siCont; the group transfected with pCMV-GL3 and siCont, pDNA+siGL3; the group transfected with pCMV-GL3 and siGL3. (A) Luciferase expression in tibialis muscle transfected with pDNA and siRNA (3 μg) using BL and US at 3 days post-transfection. * indicates P value <0.05 compared with negative control. (B) Luciferase expression in tibialis muscle transfected with pDNA and siRNA (3 μg) using BL and US at 2, 7, 14, 21 and 28 days post-transfection. * indicates P value <0.05 compared with pDNA alone. (C) Luciferase expression in skin and kidney transfected with pDNA and siRNA (3 μg) using BL and US at 3 days post-transfection.

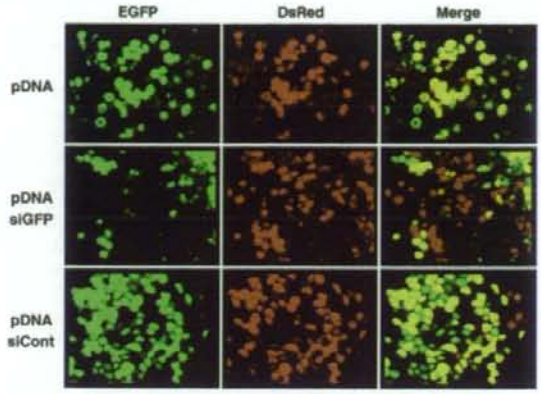

Fig. 5. Down-regulation of GFP expression by siRNA with BL and US *in vivo*. pDNA; the group transfected with pEGFP-N3 and pDsRed-N1, pDNA+siCont; the group transfected with pEGFP-N3, pDsRed-N1 and siCont, pDNA+siGFP; the group transfected with pEGFP-N3, pDsRed-N1 and siRNA targeting EGFP (siGFP). GFP and DsRed expression in tibialis muscle transfected with pDNA by electroporation 1 day before the transfection of siRNA, and transfected with siRNA (3 μg) using BL and US at 3 days post-transfection. Shown are fluorescence microscopic images of cross sections.

4. Discussion

The delivery of siRNA into specific organs *in vivo* is a major obstacle to the establishment of therapeutic RNAi. To overcome this problem, numerous transfection methods or delivery devices have been developed and reported [1–7]. The development of a targeted, nonimmunogenic siRNA delivery system for systemic administration is highly desired.

Microbubbles and US have recently been proposed for gene delivery. This combination makes sonoporation possible, allows transient changes in the permeability of the cell membrane, and makes possible the site-specific intracellular delivery of molecules such as dextran, pDNA, peptides, and siRNA both *in vitro* and *in vivo* [13–19]. However, existing microbubbles have some problems with size, stability, and targeting function. We developed novel liposomal bubbles, BL, which could be a solution to those problems. Then we reported that BL are an efficient and novel tool for gene delivery *in vitro* and *in vivo* [25–27].

Here, we investigated whether the combination of BL and US is useful for the delivery of siRNA *in vitro* and *in vivo*. We initially attempted to transfect pDNA and siRNA into COS-7 cells with BL and US. The expression of luciferase in cells was efficiently inhibited in a siRNA dose-dependent manner (Fig. 1A). Optison, one of the currently existing microbubbles, has been extensively studied [13–15,18]. The gene silencing effects of BL were equal to those of Optison (data not shown). The gene silencing effects in the siGL3-treated group persisted for at least 4 days, although the luciferase expression gradually decreased because of degradation by the nuclease and dilution due to cell division (Fig. 1B). COS-7 is well known as a cell line which efficiently expresses exogenous genes, and often used in experiments on gene

transfection. Therefore, we used it in the experiments in this study, however, we further attempted the transfection into mouse cells, NIH3T3 and C2C12. The luciferase expression was also blocked by siRNA in both cell lines (Fig. 1C). We investigated the difference in the conditions for US (intensity and duty) but found few (data not shown). When we employed US for the transfection into cells, cytotoxicity was absent after the exposure to BL (data not shown). It is important to consider the stability of the nuclease in serum for the efficient intracellular delivery of siRNA *in vivo*. We therefore examined the effects of high serum on gene silencing. As shown in Fig. 2, the down-regulation of luciferase activity by siRNA with BL was maintained in the presence of high serum. These results suggested that the transfection with BL and US was effective in serum as supported by previous findings regarding plasmid DNA delivery with BL and US [27]. In contrast, in the case of LF2000, a remarkable decrease in transfection efficiency was induced by serum. This result is consistent with reports that serum proteins interact with and disturb cationic liposomes *in vitro* and *in vivo* [28,29]. It is considered that the more time required for transfection, the greater the degradation of siRNA. Actually, the gene silencing by siRNA transfected with BL maintained about 90% efficiency even in the presence of 50% serum. However, that with LF2000 diminished to about 70% efficiency in the presence of 50% serum. We considered the difference in time required for transfection to be due to the different mechanisms of each method. Therefore, we examined the involvement of endocytosis in the process of transfection with BL and US. There was little difference in the effects of down-regulation in the presence or absence of chloroquine and at 37 °C or 4 °C (Fig. 3A and B). To evaluate the intracellular localization of siRNA transfected with BL or LF2000, we initially attempted to transfect FITC-siRNA at 25 nM into COS-7 cells. However, no fluorescence was observed even when the transfection by BL was performed with a higher concentration of siRNA, 200 nM (data not shown). We assumed that the siRNA concentrated in endosomes resulting in a too low fluorescence signal to detect. Thus, we used a signal amplification kit to enhance the fluorescence of intracellular siRNA to a detectable level. As a result, the difference in the mechanism of transfection between BL and LF2000 was shown by the intracellular distribution (Fig. 3C). In the case of transfection with LF2000, the fluorescence was distributed in a punctate pattern. This phenomenon has been observed in the endosomal pathway of lipoplex [30,31]. In contrast, the fluorescence was homogeneously dispersed mainly into the cytoplasm on transfection with BL and US for 10 s These results suggested that the transfection with BL and US did not involve endocytosis, but the siRNA was directly introduced into the cytoplasm. Thus, it seems un-necessary to consider the escape of siRNA from the endosome and the degradation of siRNA in lysosomes, because the transfection with BL and US delivers siRNA into the cytoplasm directly within a fairly short time. Although siRNAs were initially thought to be small enough to avoid activating the IFN pathway, recent studies showed that they could activate innate immunity in mammalian cells [32,33]. The immune response to siRNA was mainly induced via TLRs in the endosome [34]. Transfection with BL and US may avoids the activation of an immune response via TLRs because the siRNA enters the cytoplasm directly. For these reasons, BL could be also a useful tool *in vivo*. Indeed, when pDNA encoding luciferase and its siRNA were codelivered into the muscle of mice by BL and US, the gene expression was suppressed and the effect lasted at least 7 days (Fig. 4A and B). Gene silencing effects were also observed when siRNA was injected into skin and US was applied to the injection site, although there was no significant difference between the siGL3-treated group and untreated group due to a lack of optimization for this site (Fig. 4C). We also attempted transfection to the kidney, however, no down-regulation was observed and luciferase expression was even observed in the group transfected with pCMV-GL3 only. These results were assumed to be due to the excretion of pDNA and siRNA via the kidney [35,36]. The delivery of nucleic acids into the kidney might be difficult, unless injected by intra-renal-vascular or intra-renal-pelvic injection [37]. Although the transfection into the kidney was not effective, the transfection with BL and US was expected to enable the tissue-targeted delivery of siRNA in other organs when performed with methods suited for each organ [38]. Furthermore, the relatively stable gene expression of pDNA encoding EGFP delivered into the muscle by electroporation could be also suppressed by the intramuscular injection of siRNA and BL with exposure to US (Fig. 5). In future, we need to examine the endogenous gene silencing effects of siRNA transfected with BL and US.

These results suggest that BL are a useful tool for the delivery of siRNA as well as that of pDNA *in vitro* and *in vivo*. BL are smaller than conventional microbubbles [26,27]. Thus, BL could be delivered deep into the tissue and expected to achieve therapeutic effects. However, all data were obtained using a mixture of BL and naked siRNA in this study. With systemic injections, it is important to control the biodistribution of both BL and siRNA. In addition, the delivery of siRNA has obstacles such as nuclease degradation and a rapid removal from the circulation after intravenous administration. Therefore, to resolve these issues, we are attempting to prepare a siRNA-entrapping type or complex type of BL using cationic lipid. Recently, microbubbles conjugated to an antibody and having a targeting function have been developed [39–41]. Liposomes can be easily modified to add a targeting function. We are also attempting to develop targeting BL using antibody or peptide. In this study, we showed the combination of BL and US to be an effective and novel siRNA delivery method *in vitro* and *in vivo*.

Acknowledgements

We are grateful to Dr. Katsuro Tachibana (Department of Anatomy, School of Medicine, Fukuoka University) for technical advice regarding the induction of cavitation with US, to Ms. Kazumi Ishii, Ms. Miyuki Ozawa, Ms. Kana Kubota, and Ms. Yuko Ishii (School of Pharmacy, Tokyo University of Pharmacy and Life Sciences) for excellent technical assistance, and to Mr. Yasuhiko Hayakawa, Mr. Takahiro Yamauchi, and Mr. Kosho Suzuki (NEPA GENE CO., LTD.) for technical advice regarding exposure to US. This study was supported by an Industrial Technology Research Grant (04A05010) from the New Energy and Industrial Technology Development Organization (NEDO) of Japan and a Grant-in-aid for Exploratory Research (18650146) from the Japan Society for the Promotion of Science.

References

[1] J.D. Hommel, R.M. Sears, D. Georgescu, D.L. Simmons, R.J. DiLeone, Local gene knockdown in the brain using viral-mediated RNA interference, Nat. Med. 9 (2003) 1539–1544.
[2] Q. Ge, L. Filip, A. Bai, T. Nguyen, H.N. Eisen, J. Chen, Inhibition of influenza virus production in virus-infected mice by RNA interference, Proc. Natl. Acad. Sci. U. S. A. 101 (2004) 8676–8681.
[3] E. Song, S.K. Lee, J. Wang, N. Ince, N. Ouyang, J. Min, J. Chen, P. Shankar, J. Lieberman, RNA interference targeting Fas protects mice from fulminant hepatitis, Nat. Med. 9 (2003) 347–351.
[4] J. Soutschek, A. Akinc, B. Bramlage, K. Charisse, R. Constien, M. Donoghue, S. Elbashir, A. Geick, P. Hadwiger, J. Harborth, M. John, V. Kesavan, G. Lavine, R.K. Pandey, T. Racie, K.G. Rajeev, I. Rohl, I. Toudjarska, G. Wang, S. Wuschko, D. Bumcrot, V. Koteliansky, S. Limmer, M. Manoharan, H.P. Vornlocher, Therapeutic silencing of an endogenous gene by systemic administration of modified siRNAs, Nature 432 (2004) 173–178.
[5] B. Urban-Klein, S. Werth, S. Abuharbeid, F. Czubayko, A. Aigner, RNAi-mediated gene-targeting through systemic application of polyethylenimine (PEI)-complexed siRNA in vivo, Gene Ther. 12 (2005) 461–466.
[6] J. Yano, K. Hirabayashi, S. Nakagawa, T. Yamaguchi, M. Nogawa, I. Kashimori, H. Naito, H. Kitagawa, K. Ishiyama, T. Ohgi, T. Irimura, Antitumor activity of small interfering RNA/cationic liposome complex in mouse models of cancer, Clin. Cancer Res. 10 (2004) 7721–7726.
[7] M. Golzio, L. Mazzolini, P. Moller, M.P. Rols, J. Teissie, Inhibition of gene expression in mice muscle by in vivo electrically mediated siRNA delivery, Gene Ther. 12 (2005) 246–251.
[8] R.P. Holmes, L.D. Yeaman, R.G. Taylor, D.L. McCullough, Altered neutrophil permeability following shock wave exposure in vitro, J. Urol. 147 (1992) 733–737.
[9] M. Delius, G. Adams, Shock wave permeabilization with ribosome inactivating proteins: a new approach to tumor therapy, Cancer Res. 59 (1999) 5227–5232.
[10] W.J. Greenleaf, M.E. Bolander, G. Sarkar, M.B. Goldring, J.F. Greenleaf, Artificial cavitation nuclei significantly enhance acoustically induced cell transfection, Ultrasound Med. Biol. 24 (1998) 587–595.

[11] P. Schratzberger, J.G. Krainin, G. Schratzberger, M. Silver, H. Ma, M. Kearney, R.F. Zuk, A.F. Brisken, D.W. Losordo, J.M. Isner, Transcutaneous ultrasound augments naked DNA transfection of skeletal muscle, Mol. Ther. 6 (2002) 576–583.
[12] M. Duvshani-Eshet, M. Machluf, Therapeutic ultrasound optimization for gene delivery: a key factor achieving nuclear DNA localization, J. Control. Release 108 (2005) 513–528.
[13] Y. Taniyama, K. Tachibana, K. Hiraoka, M. Aoki, S. Yamamoto, K. Matsumoto, T. Nakamura, T. Ogihara, Y. Kaneda, R. Morishita, Development of safe and efficient novel nonviral gene transfer using ultrasound: enhancement of transfection efficiency of naked plasmid DNA in skeletal muscle, Gene Ther. 9 (2002) 372–380.
[14] Y. Taniyama, K. Tachibana, K. Hiraoka, T. Namba, K. Yamasaki, N. Hashiya, M. Aoki, T. Ogihara, K. Yasufumi, R. Morishita, Local delivery of plasmid DNA into rat carotid artery using ultrasound, Circulation 105 (2002) 1233–1239.
[15] T. Li, K. Tachibana, M. Kuroki, M. Kuroki, Gene transfer with echo-enhanced contrast agents: comparison between Albunex, Optison, and Levovist in mice-initial results, Radiology 229 (2003) 423–428.
[16] E.C. Unger, T. Porter, W. Culp, R. Labell, T. Matsunaga, R. Zutshi, Therapeutic applications of lipid-coated microbubbles, Adv. Drug Deliv. Rev. 56 (2004) 1291–1314.
[17] S. Sonoda, K. Tachibana, E. Uchino, A. Okubo, M. Yamamoto, K. Sakoda, T. Hisatomi, K.H. Sonoda, Y. Negishi, Y. Izumi, S. Takao, T. Sakamoto, Gene transfer to corneal epithelium and keratocytes mediated by ultrasound with microbubbles, Invest. Ophthalmol. Vis. Sci. 47 (2006) 558–564.
[18] M. Kinoshita, K. Hynynen, A novel method for the intracellular delivery of siRNA using microbubble-enhanced focused ultrasound, Biochem. Biophys. Res. Commun. 335 (2005) 393–399.
[19] S. Tsunoda, O. Mazda, Y. Oda, Y. Iida, S. Akabame, T. Kishida, M. Shin-Ya, H. Asada, S. Gojo, J. Imanishi, H. Matsubara, T. Yoshikawa, Sonoporation using microbubble BR14 promotes pDNA/siRNA transduction to murine heart, Biochem. Biophys. Res. Commun. 336 (2005) 118–127.
[20] G. Blume, G. Cevc, Liposomes for the sustained drug release in vivo, Biochim. Biophys. Acta. 1029 (1990) 91–97.
[21] T.M. Allen, C. Hansen, F. Martin, C. Redemann, A. Yau-Young, Liposomes containing synthetic lipid derivatives of poly(ethylene glycol) show prolonged circulation half-lives in vivo, Biochim. Biophys. Acta. 1066 (1991) 29–36.
[22] K. Maruyama, T. Yuda, A. Okamoto, S. Kojima, A. Suginaka, M. Iwatsuru, Prolonged circulation time in vivo of large unilamellar liposomes composed of distearoyl phosphatidylcholine and cholesterol containing amphipathic poly(ethylene glycol), Biochim. Biophys. Acta. 1128 (1992) 44–49.
[23] K. Maruyama, O. Ishida, S. Kasaoka, T. Takizawa, N. Utoguchi, A. Shinohara, M. Chiba, H. Kobayashi, M. Eriguchi, H. Yanagie, Intracellular targeting of sodium mercaptoundecahydrododecaborate (BSH) to solid tumors by transferrin-PEG liposomes, for boron neutron-capture therapy (BNCT), J. Control. Release 98 (2004) 195–207.
[24] M. Harata, Y. Soda, K. Tani, J. Ooi, T. Takizawa, M. Chen, Y. Bai, K. Izawa, S. Kobayashi, A. Tomonari, F. Nagamura, S. Takahashi, K. Uchimaru, T. Iseki, T. Tsuji, T.A. Takahashi, K. Sugita, S. Nakazawa, A. Tojo, K. Maruyama, S. Asano, CD19-targeting liposomes containing imatinib efficiently kill Philadelphia chromosome-positive acute lymphoblastic leukemia cells, Blood 104 (2004) 1442–1449.
[25] R. Suzuki, T. Takizawa, Y. Negishi, K. Hagisawa, K. Tanaka, K. Sawamura, N. Utoguchi, T. Nishioka, K. Maruyama, Gene delivery by combination of novel liposomal bubbles with perfluoropropane and ultrasound, J. Control. Release 117 (2007) 130–136.
[26] R. Suzuki, T. Takizawa, Y. Negishi, N. Utoguchi, K. Sawamura, K. Tanaka, E. Namai, Y. Oda, Y. Matsumura, K. Maruyama, Tumor specific ultrasound enhanced gene transfer in vivo with novel liposomal bubbles, J. Control. Release 125 (2008) 137–144.
[27] R. Suzuki, T. Takizawa, Y. Negishi, N. Utoguchi, K. Maruyama, Effective gene delivery with novel liposomal bubbles and ultrasonic destruction technology, Int. J. Pharm. 354 (2008) 49–55.
[28] S.E. Han, H. Kang, G.Y. Shim, M.S. Suh, S.J. Kim, J.S. Kim, Y.K. Oh, Novel cationic cholesterol derivative-based liposomes for serum-enhanced delivery of siRNA, Int. J. Pharm. 353 (2008) 260–269.
[29] M. Furuhata, H. Kawakami, K. Toma, Y. Hattori, Y. Maitani, Design, synthesis and gene delivery efficiency of novel oligo-arginine-linked PEG-lipids: effect of oligo-arginine length, Int. J. Pharm. 316 (2006) 109–116.
[30] E.G. Marcusson, B. Bhat, M. Manoharan, C.F. Bennett, N.M. Dean, Phosphorothioate oligodeoxyribonucleotides dissociate from cationic lipids before entering the nucleus, Nucleic Acids Res. 26 (1998) 2016–2023.
[31] L. Tonges, P. Lingor, R. Egle, G.P. Dietz, A. Fahr, M. Bahr, Stearylated octaarginine and artificial virus-like particles for transfection of siRNA into primary rat neurons, RNA 12 (2006) 1431–1438.
[32] S.M. Elbashir, J. Harborth, W. Lendeckel, A. Yalcin, K. Weber, T. Tuschl, Duplexes of 21-nucleotide RNAs mediate RNA interference in cultured mammalian cells, Nature 411 (2001) 494–498.
[33] C.A. Sledz, M. Holko, M.J. de Veer, R.H. Silverman, B.R. Williams, Activation of the interferon system by short-interfering RNAs, Nat. Cell. Biol. 5 (2003) 834–839.
[34] M. Sioud, RNA interference and innate immunity, Adv. Drug Deliv. Rev. 59 (2007) 153–163.
[35] N. Kobayashi, T. Kuramoto, K. Yamaoka, M. Hashida, Y. Takakura, Hepatic uptake and gene expression mechanisms following intravenous administration of plasmid DNA by conventional and hydrodynamics-based procedures, J. Pharmacol. Exp. Ther. 297 (2001) 853–860.
[36] P.Y. Lu, F. Xie, M.C. Woodle, In vivo application of RNA interference: from functional genomics to therapeutics, Adv. Genet. 54 (2005) 117–142.
[37] L.W. Lai, G.W. Moeckel, Y.H. Lien, Kidney-targeted liposome-mediated gene transfer in mice, Gene Ther. 4 (1997) 426–431.
[38] S. Chen, J.H. Ding, R. Bekeredjian, B.Z. Yang, R.V. Shohet, S.A. Johnston, H.E. Hohmeier, C.B. Newgard, P.A. Grayburn, Efficient gene delivery to pancreatic islets with ultrasonic microbubble destruction technology, Proc. Natl. Acad. Sci. U. S. A. 103 (2006) 8469–8474.
[39] H. Leong-Poi, J. Christiansen, P. Heppner, C.W. Lewis, A.L. Klibanov, S. Kaul, J.R. Lindner, Assessment of endogenous and therapeutic arteriogenesis by contrast ultrasound molecular imaging of integrin expression, Circulation 111 (2005) 3248–3254.
[40] C.Z. Behm, B.A. Kaufmann, C. Carr, M. Lankford, J.M. Sanders, C.E. Rose, S. Kaul, J.R. Lindner, Molecular imaging of endothelial vascular cell adhesion molecule-1 expression and inflammatory cell recruitment during vasculogenesis and ischemia-mediated arteriogenesis, Circulation 117 (2008) 2902–2911.
[41] M. Palmowski, J. Huppert, G. Ladewig, P. Hauff, M. Reinhardt, M.M. Mueller, E.C. Woenne, J.W. Jenne, M. Maurer, G.W. Kauffmann, W. Semmler, F. Kiessling, Molecular profiling of angiogenesis with targeted ultrasound imaging: early assessment of antiangiogenic therapy effects, Mol. Cancer Ther. 7 (2008) 101–109.